

AD-A191 084

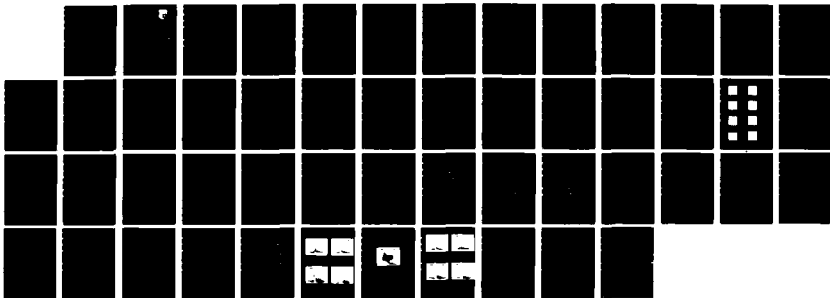
LASER COMPARISON STUDY OF ND:BEL AND ND:YAG(U) AIR  
FORCE WRIGHT AERONAUTICAL LABS WRIGHT-PATTERSON AFB OH  
R C SIMPSON OCT 87 AFMAL-TR-87-1138

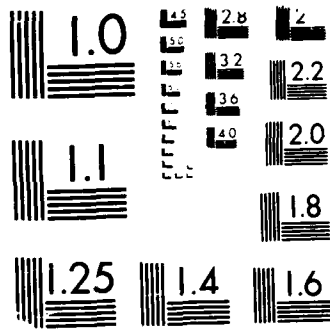
1/1

UNCLASSIFIED

F/G 9/3

ML





MICROCOPY RESOLUTION TEST CHART  
NATIONAL BUREAU OF STANDARDS-1963-A

DTIC FILE COPY



# Laser Comparison Study of Nd:BEL and Nd:YAG

Lt Ralph C. Simpson  
Electro-Optic Sources Group  
Electro-Optic Technology Branch

DTIC  
ELECTE  
FEB 05 1988  
S D

Final Report for Period December 1985 - June 1986

30 October 1986

Approved for public release: distribution unlimited

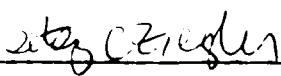
AVIONICS LABORATORY  
AIR FORCE WRIGHT AERONAUTICAL LABORATORIES  
AIR FORCE SYSTEMS COMMAND  
WRIGHT PATTERSON AIR FORCE BASE, OHIO 45433-6543

NOTICE

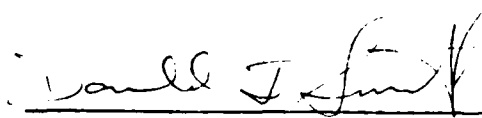
When Government drawings, specifications, or other data are used for any purpose other than in connection with a definitely Government-related procurement, the United States Government incurs no responsibility or any obligation whatsoever. The fact that the Government may have formulated or in any way supplied the said drawings, specifications, or other data, is not to be regarded by implication, or otherwise in any manner construed, as licensing the holder, or any other person or corporation; or as conveying any rights or permission to manufacture, use, or sell any patented invention that may in any way be related thereto.

This report has been reviewed by the Office of Public Affairs (ASD/PA) and is releasable to the National Technical Information Service (NTIS). At NTIS, it will be available to the general public, including foreign nations.

This technical report has been reviewed and is approved for publication.



Lt Betsy C. Ziegler  
Electro-Optic Sources Group  
Electro-Optic Technology Branch



Donald Smith  
Electro-Optic Sources Group  
Electro-Optic Technology Branch

FOR THE COMMANDER



Richard Renski  
Electro-Optics Technology Branch  
Electronic Technology Division

If your address has changed, if you wish to be removed from our mailing list, or if the addressee is no longer employed by your organization please notify AFWAL/AADO-1, Wright-Patterson AFB, OH 45433-6543 to help us maintain a current mailing list.

Copies of this report should not be returned unless return is required by security considerations, contractual obligations, or notice on a specific document.

A191024

## REPORT DOCUMENTATION PAGE

1a. REPORT SECURITY CLASSIFICATION Unclassified		1b. RESTRICTIVE MARKINGS N/A	
2a. SECURITY CLASSIFICATION AUTHORITY N/A		3. DISTRIBUTION/AVAILABILITY OF REPORT Approved for public release; distribution unlimited	
2b. DECLASSIFICATION/DOWNGRADING SCHEDULE N/A		4. PERFORMING ORGANIZATION REPORT NUMBER(S) AFWAL-TR-87-1130	
4. PERFORMING ORGANIZATION REPORT NUMBER(S) AFWAL-TR-87-1130		5. MONITORING ORGANIZATION REPORT NUMBER(S)	
6a. NAME OF PERFORMING ORGANIZATION Air Force Wright Aeronautical Laboratories	6b. OFFICE SYMBOL (If applicable) AADO-1	7a. NAME OF MONITORING ORGANIZATION	
6c. ADDRESS (City, State and ZIP Code) WPAFB OH 45433-6543		7b. ADDRESS (City, State and ZIP Code)	
8a. NAME OF FUNDING/SPONSORING ORGANIZATION Avionics Laboratory	8b. OFFICE SYMBOL (If applicable) AADO-1	9. PROCUREMENT INSTRUMENT IDENTIFICATION NUMBER N/A	
8c. ADDRESS (City, State and ZIP Code) WPAFB OH 45433-6543		10. SOURCE OF FUNDING NOS.	
11. TITLE (Include Security Classification) Laser Comparison Study of Nd:BEL and Nd:YAG		PROGRAM ELEMENT NO. 62204F	PROJECT NO. 2001
		TASK NO. 05	WORK UNIT NO. 01
12. PERSONAL AUTHOR(S) Lt Ralph C. Simpson			
13a. TYPE OF REPORT Final	13b. TIME COVERED FROM Dec 85 to Jun 86	14. DATE OF REPORT (Yr., Mo., Day) 1987 October	15. PAGE COUNT 52
16. SUPPLEMENTARY NOTATION Performed as part of The Technology Cooperation Program (TTCP) under Joint Technology Panel 10 (JTP 10 - laser technology)			
17. COSATI CODES		18. SUBJECT TERMS (Continue on reverse if necessary and identify by block number)	
FIELD	GROUP	SUB. GR.	
20	05	Nd:YAG	
20	06	Nd:BEL	
		Solid State Laser	
19. ABSTRACT (Continue on reverse if necessary and identify by block number) This report describes a performance comparison between the solid state laser materials Nd:BEL and Nd:YAG using 6.35X66.67 mm rods; four basic measurements were conducted: 1) energy input vs energy output 2) beam divergence 3) pulse to pulse stability and 4) pulse width. Relative performance was evaluated to help determine the feasibility of using Nd:BEL as a laser source.			
20. DISTRIBUTION/AVAILABILITY OF ABSTRACT UNCLASSIFIED/UNLIMITED <input checked="" type="checkbox"/> SAME AS RPT. <input type="checkbox"/> DTIC USERS <input type="checkbox"/>		21. ABSTRACT SECURITY CLASSIFICATION Unclassified	
22a. NAME OF RESPONSIBLE INDIVIDUAL Lt Betsy C. Ziegler		22b. TELEPHONE NUMBER (Include Area Code) (513)255-3804	22c. OFFICE SYMBOL AFWAL/AADO-1

## FOREWORD

The work reported herein was performed during the period 23 December 1985 to 13 June 1986, by 1Lt Ralph C. Simpson (AFWAL/AADO-1), project scientist. The report was released by the author in August 1986. The author wishes to thank Dr. Ken Schepler (AFWAL/AADO-1) for his invaluable technical assistance and proofreading, the Laser/Electro-Optical Branch of Aeronautical Systems Division for the supply of Nd:YAG laser rods, the Electro-Optic Technology Branch of the Air Force Wright Aeronautical Laboratories for facility and funding support, and the Australian government for the supply of Nd:BEL rods.

This report is dedicated to the memory of Dr. Wolfgang Schuebel whose efforts made this research possible.

TABLE OF CONTENTS

SECTION	PAGE
I INTRODUCTION .....	1
II BACKGROUND .....	2
1. Nd:YAG Properties .....	2
2. Nd:BEL Properties .....	2
III EXPERIMENTAL PROCEDURE .....	4
1. Laboratory Set Up .....	4
2. Measurement Methods .....	5
IV RESULTS .....	8
1. Energy Input vs. Energy Output .....	8
2. Beam Divergence .....	10
3. Pulse to Pulse Stability .....	11
4. Pulse Width .....	11
V DISCUSSION AND CONCLUSIONS .....	13
REFERENCES .....	15

Accession For	
NBS DTIC	✓
DTIC TAB	<input type="checkbox"/>
Unannounced	<input type="checkbox"/>
Justification	
By	
Date	
Approved by	
Dist	
A-1	

SECTION I  
INTRODUCTION

Except for a few early instances, military tactical lasers have used Nd<sup>3+</sup> doped Y<sub>3</sub>Al<sub>5</sub>O<sub>12</sub> (Nd:YAG) as the laser material. With an output wavelength of 1.064  $\mu$ m and an optimum slope efficiency near 3.0%, the performance of this solid state material is well known (1), while the use of other materials is currently being evaluated (2,3,4). To provide an advantage over Nd:YAG, issues such as efficiency, beam quality, reliability, and availability must be considered.

A study of a possible alternative to Nd:YAG was undertaken. Nd<sup>3+</sup> doped La<sub>2</sub>Be<sub>2</sub>O<sub>5</sub> (Nd:BEL) was the material that was chosen. The research concentrated on relative performance parameters. What we hoped to identify were any glaring weaknesses of a material which would preclude its military use, or any significant strengths which would encourage its exploitation. To complement the data obtained, a brief discussion of spectroscopy, lasing levels, and other physical properties is included in Section II. (solid state laser)

Initially the comparison studies were to be made by using a PAVE NAIL laser transmitter as the evaluation standard. Data was taken with Nd:YAG and Nd:BEL alternately housed in the laser cavity. Unfortunately the transmitter failed to work consistently in the laboratory and repair facilities were not readily available. Therefore another method had to be identified. The test set up that was used is described in Section III. This method did not provide a baseline comparison using a military system, but it did allow for expanded measurements such as varied repetition rates and electro-optic Q-switching.

## SECTION II

### BACKGROUND

#### 1. Nd:YAG PROPERTIES

Nd:YAG has been used extensively for commercial and military applications. Its low lasing threshold, high damage threshold, and high stimulated emission cross section have made it the material to which new crystals are compared.

$\text{Y}_3\text{Al}_5\text{O}_{12}$  (YAG) is a cubic crystal with high thermal conductivity as shown in Table 1. The  ${}^4\text{F}_{3/2} \rightarrow {}^4\text{I}_{11/2}$  transition of  $\text{Nd}^{3+}$  is the strongest with a stimulated emission cross section of  $4.6 \times 10^{-19} \text{ cm}^2$  and a fluorescence lifetime of 230  $\mu\text{s}$  [5]. The nominal output wavelength is 1.064  $\mu\text{m}$ .

The Nd:YAG rods used in this research were doped at 1.0 - 1.1 at. % Nd. The fluorescence spectrum of a Nd:YAG rod is shown in Figure 1. The data was taken with a 1.26 m Spex spectrometer.

#### 2. Nd:BEL PROPERTIES

The fluorescence spectrum of Nd:BEL in the 1.0  $\mu\text{m}$  region is also shown in Figure 1. The first lasing action of Nd:BEL was obtained by Morris et al [6] in 1975. Subsequent work [7] yielded much data on its basic properties and provided the baseline for further investigations.

$\text{La}_2\text{Be}_2\text{O}_5$  is a monoclinic crystal with low site symmetry. Consequently all  $\text{Nd}^{3+}$  transitions are possible, but they are polarization dependent. Two of the stronger transitions are at 1.070 and 1.079  $\mu\text{m}$ . The 1.070  $\mu\text{m}$  transition has its greatest stimulated emission cross section along the x vibration axis at  $2.1 \times 10^{-19} \text{ cm}^2$ , and the value for the 1.079  $\mu\text{m}$  transition is greatest along the y axis at  $1.5 \times 10^{-19} \text{ cm}^2$  [7]. Judging by this information it stands to reason that the output of a Nd:BEL rod will depend on how it is cut and its orientation in the optical cavity.

As can be seen in the absorption spectra taken with a Cary 14 spectrophotometer in Figures 2 and 3, Nd:BEL has much broader absorption lines than Nd:YAG, but a similar peak absorption cross section. This theoretically allows for more efficient pumping. The fluorescence lifetime of the  ${}^4F_{3/2}$  level is 150  $\mu$ s, or 65% of the Nd:YAG value.

Various physical properties are listed in Table 1. A past disadvantage of BEL has been poor performance related to thermal lensing and birefringence. In order to alleviate the variance in resonator length due to rod temperature, research is being conducted on the use of an athermal cut of Nd:BEL [2]. The rod used in this research was an x-axis cut rod (E parallel to y polarization).

SECTION III  
EXPERIMENTAL PROCEDURE

1. LABORATORY SET UP

a. Resonator Cavity

The unique size of the laser rods provided by the Pave Nail transmitters (6.35 x 66.67 mm) required the fabrication of a non-standard rod and flashlamp housing. To accomplish this, Kigre Inc., altered an FC-20K cavity to hold a 53.97 mm arc length ILC flashlamp (Model 5782) and the host material. Cooling was maintained at 22° C by a Neslab RTE-4 circulating cooler filled with deionized water.

Figure 4 details a schematic of the set up used and Table II lists the equipment. The basic resonator consisted of a 3 m radius of curvature HR mirror and a flat 50% outcoupling mirror. These were approximately 64 cm apart, with the laser cavity in the middle. For YAG Q-switched operation and long pulse 1.08  $\mu\text{m}$  lasing of BEL, a polarizer was placed between the rod and HR mirror. For BEL Q-switched operation, an Inrad Model 202 Q-switch was inserted between the HR mirror and laser cavity, for YAG it was put between the polarizer and the HR mirror. All resonator components were mounted on a Gaertner optical bench. Optical alignment was accomplished by using a HeNe laser.

b. Pulse Forming Network

Pulsing of the laser was controlled by a PAL Kit Co. pulse generator which controlled a Candela Corp. FD-100 flashlamp driver and HVD 250-A power supply. The system could be operated on manual trigger or at repetition rates of 1 or 10 Hz. Flashlamp pulse widths were nominally 200  $\mu\text{s}$  at FWHM. Q-switch operation was driven by an INRAD 2-016 Q-switch driver.

c. Measurement Equipment

All energy measurements were accomplished by using a Laser Precision

RJP 735 probe and Rj 7200 ratiometer in combination with neutral density filters. Wavelength measurements were obtained by using a .5 m Jarrell-Ash monochromator. Pulse shape data was gathered by using either a Lite Mike detector or a Si photodiode with one of two Tektronix oscilloscopes. One of the oscilloscopes was digital and its output could be transferred to a Moseley X-Y recorder.

## 2. MEASUREMENT METHODS

Comparison investigations consisted of four basic measurements: 1) Energy Input vs. Energy Output ( $E_{in}$  vs.  $E_{out}$ ), 2) beam divergence, 3) pulse to pulse stability and 4) pulse width. These were obtained for long pulse and Q-switched operation at 1 Hz and 10 Hz, and at varying input energies.

### a. $E_{in}$ vs. $E_{out}$

For energy measurements it was necessary to attenuate the output beam to avoid damage to the detector. To accomplish this a combination of neutral density filters was used. Nominally rated at optical densities of .5 and 1.0 for 532 nanometer output, their OD values for a 1.06 - 1.08  $\mu\text{m}$  output had to be calculated. This was done by taking energy measurements for varying combinations of filters and using the following relationship:

Let  $E_x$  = Energy detected using one .5 OD filter

$E_y$  = Energy detected using two .5 OD filters

Therefore  $E_x = 10^{-\alpha} \cdot E_y$  where  $\alpha$  = optical density of .5 OD filter at 1  $\mu\text{m}$

Let  $E_z$  = Energy detected using 1.0 and .5 OD filter combination

Therefore  $E_y = 10^{-\beta} \cdot E_z$  where  $\beta$  = optical density of 1.0 OD filter at 1  $\mu\text{m}$

Data gathered over a wide range of output energies yielded:

$$\alpha = .69 \pm .02 \quad (\text{for both .5 OD filters})$$

$$\beta = .72 \pm .02$$

To verify that the optical densities were so similar in value, their transmission spectra were measured on a Cary 14 spectrophotometer. The

optical densities were indeed similar, with the attenuation of 1.0 OD filter being only slightly higher than the .5 OD filter. It was then possible to establish the following conversion factors for readings obtained while using different filter combinations:

two .5 OD filters: 24.0 x detector reading

1.0 and .5 OD filter combination: 25.7 x detector reading

one 1.0 OD and two .5 OD filters combination: 125.9 x detector reading

For the purpose of consistency and ease of presentation all  $E_{in}$  vs.  $E_{out}$  results shown in this report were obtained using the two .5 filter combination unless indicated otherwise.

b. Beam divergence

The method used to obtain beam divergence does not yield an absolute divergence value. Accurate measurement of beam divergence requires careful measurement and control of beam profile. Typically, it is necessary to produce a far field beam pattern and the corresponding data is based on the assumption of a Gaussian beam ( $TEM_{00}$ ). Since there was only an interest in comparative performance and since the beam profile was multimode and not Gaussian, a very simple method was used.

Zap-it paper was placed at varying distances from the output mirror. An impression of the beam shape was created as shown in Figure 5. The diameter of the spot was then measured and plotted as a function of distance for a given input energy, repetition rate, and pulse mode. For the cases where an elliptical image was produced, a major (Y) and minor (X) axis were defined and one plot was made for each axis. By performing a linear regression on these plots, "divergence" values were obtained. A performance analysis of the two different hosts is made possible by comparing these values at different input energies, and operational modes.

c. Pulse to pulse stability

Pulse to pulse stability measurements were obtained by reflecting the output beam off of a Lambertian surface then detecting it with a Lite Mike detector. The detector output was recorded on a digital oscilloscope which was read out to an X-Y recorder. To prevent detector saturation the beam was attenuated.

At 1 Hz operation the tenth laser pulse produced was stored on the oscilloscope and read out to the recorder. This procedure was repeated five times for a given input energy. At 10 Hz operation a sample pulse was stored after approximately ten seconds of operation. This was also done five times for a given input energy.

For long pulse output the X-Y recorder plotted a curve as is shown in Figure 6a. The area under the curve represents the energy detected, and for different pulses this value will vary. To measure this variance, or pulse to pulse stability, each curve was cut away with scissors, then weighed to the nearest .1 milligram. For each input energy, the integrated curves were calibrated to a previously measured average output energy. Finally, a graph was made of energy deviation from the average for each pulse sample.

For Q-switched operation the X-Y recorder plot was quite narrow (see Figure 6b) and the peaks were merely calibrated to an average energy. Once again, a plot was produced of energy variance for each sample.

d. Pulse width

Pulse width measurements were obtained by using a Lambertian reflector and a Si photodiode. The output was then stored and photographed. Response time limitations of the detection system did not allow for accurate measurements of pulse widths below 25-35 ns.

SECTION IV  
COMPARISON RESULTS

1. ENERGY INPUT VS. ENERGY OUTPUT

a. Long Pulse at 1 Hz

Energy readings were obtained by averaging ten pulses and repeating this procedure five times. The final value was then calculated by averaging these five data points.

Results of long pulse Nd:YAG  $E_{in}$  vs.  $E_{out}$  for 1 Hz operation are shown in Figure 7. The slope efficiency of Run I is 5.2%. This seemed quite high for this material, so to verify the results the measurements were repeated with a different rod and are graphed as Run II. The slope efficiency of this plot is 4.8%, which is consistent with Run I.

Nd:BEL energy efficiency is plotted with the Run I YAG data in Figure 8. The output of the BEL was polarized and was at a wavelength of 1079 nm. ( $\approx 1.08 \mu\text{m}$ ). The measured slope efficiency was 3.4%. As can be seen from the graph, the YAG demonstrated a lower threshold and a higher slope efficiency. Saturation was not observed for either rod at these pumping levels.

An attempt was also made at lasing the BEL material at the 1.07  $\mu\text{m}$  line. A Calcite polarizer was inserted in the cavity and the components aligned to produce 1.08  $\mu\text{m}$  and 1.07  $\mu\text{m}$  radiation. Results are shown in Figures 9 and 10. As is to be expected from the way the rod was cut, the 1.08  $\mu\text{m}$  output was substantially higher than the 1.07  $\mu\text{m}$  output. Slope efficiencies were 1.6% and .10% respectively. The decrease in efficiency for the 1.08  $\mu\text{m}$  output can be attributed to losses induced by the polarizer.

b. Long Pulse at 10 Hz

Performance comparison of the two materials for long pulse lasing at 10 Hz is shown in Figure 11. The YAG rod again demonstrated a lower lasing

threshold, but unlike the 1 Hz data, BEL exhibited a slightly higher slope efficiency than YAG, 5.1% vs. 4.8%. This was not due to a decrease in YAG performance, but rather to a 67% increase in the BEL performance. The possible cause for this is presented in Section V.

The YAG output showed some saturation as can be seen in the slight rollover on the graph. The BEL output remained linear. Increased pumping was not possible because the power supply could not provide more energy at 10 Hz.

c. 1 Hz Q-switching

Nd:BEL showed better performance vs. YAG for 1 Hz Q-switching as is shown in Figure 12. The lasing thresholds were similar, however BEL slope efficiency was at 1.3% and Nd:YAG was at .9%. The efficiency calculation for the YAG rod was based on output before the rollover as saturation is clearly observed. BEL showed only minimal saturation.

The BEL data was taken with a three neutral density filter scheme to avoid damage to the energy detector, and because its output was naturally polarized, a polarizer was not needed in the resonator cavity. This was not the case for YAG. To estimate the loss introduced by the thin film polarizer Nd:BEL was operated with the polarizer in the cavity and the plot is also shown in Figure 12. The slope efficiency was 1.02%, so it had little impact on that parameter, but a decrease in wallplug efficiency is easily seen on the graph. This was obviously due to a fixed insertion loss introduced by the polarizer.

d. 10 Hz Q-switching

Figure 13 shows the comparison for 10 Hz Q-switched operation. Aside from a decrease in wallplug efficiency for both rods, the results were similar to the 1 Hz lasing. Slope efficiencies were 1.1% for BEL and .9% for YAG. Saturation was seen in the YAG but not in the BEL.

It should be mentioned that both materials sustained damage to their anti reflective coatings after prolonged operation at 10 Hz with Q-switching. No significant difference in the level of damage was apparent.

## 2. BEAM DIVERGENCE

### a. Long Pulse at 1 Hz

Using the method described in Section III, divergence data was collected and the resulting graph is shown in Figure 14. The images for Nd:YAG were circular throughout the input energy range and the divergence values were a nearly constant 2.5 mrad. The BEL images were always elliptical, with the X axis divergence being very nearly identical to the YAG divergence and the Y axis divergence showing higher values at higher input energies. 10 Hz long pulse divergence data was not obtained.

### b. 1 Hz Q-switching

Graphed in Figures 15 and 16 are the divergence results for 1 Hz Q-switching. Again the YAG material showed less elliptical output. The X axis divergence did not reveal a consistent pattern. There was a decrease, then an increase in divergence values after several equal values at lower pumping energies. The Nd:BEL material maintained an elliptical output. The X axis divergence showed a steady, but not drastic, increase with increasing input energy. The Y axis divergence demonstrated inconsistent behavior. Like the YAG, its initial values were fairly equal, but beyond 18 J it increased, then decreased.

For both rods the divergence of Q-switched pulses was less than the long pulse results at similar input energies. Both materials also demonstrated a decrease and then an increase in divergence after fairly constant values at lower pumping energies, with the YAG results being more dramatic. Section V puts forth possible explanations for this behavior.

c. Q-switched at 10 Hz

At 10 Hz Q-switching both materials had elliptical outputs throughout. Figures 17 and 18 show that the YAG had greater divergence than the BEL.

Y axis results show the value for YAG steadily increasing to 4.3 mrad then sharply decreasing to 3.3 mrad. This is comparable to BEL's performance but more exaggerated, as the BEL leveled off somewhat at 2.5 mrad before decreasing.

The X axis plot shows similar behavior. The divergence values were lower, but YAG again had a definite increase followed by a decrease, and the BEL leveled off before decreasing at its highest input energy.

### 3. PULSE TO PULSE STABILITY

Figures 19 through 24 show the results for pulse to pulse stability. As can be seen, no drastic variations were observed for any of the measurements. Figure 25 shows the variations in output energy maximum to minimum, and again no major deviations are observed. The long pulse results do show some variation, but it must be remembered that the method used involved some error (paper cutting).

It was necessary to obtain a pulse shape versus simple energy readings to determine if any spurious spikes were present in a laser's output. This type of behavior was only observed with 1 Hz Q-switching of Nd:BEL at 17 J pumping. Figure 6c shows a pulse sample with this type of output. It was plotted as pulse number five in Figure 21, and it does not show substantial energy variance as determined from its peak.

### 4. PULSE WIDTH

a. 1 Hz Q-switching

The pulse widths for BEL and YAG at two different energy inputs are shown in Figure 26. A FWHM reading for YAG yields 35 ns at 10.8 J input and 45 ns at 13.8 J. Because of the equipment response time limitations

mentioned in Section III, the actual pulse width at 10.8 J pumping may have been lower than 35 ns. The pulse width for 12 J input is probably near 45 ns. Since a large increase in pulse width is not likely for only a 2.8 J increase in pumping, (in fact one would expect a decrease), the 35 ns pulse width measurement is probably not too far off.

BEL showed much wider pulse widths. At 10.8 J input the pulse width was approximately 100 ns and at 13.8 J input it was also 100 ns. Because there was no reason to believe BEL would have such wide pulse widths, measurements were repeated and greater care was taken to avoid detector saturation. The result for an input energy of 10.8 J is shown in Figure 27. A FWHM reading yields a pulse width near 45 ns which is comparable to the YAG result. Thus the wider BEL Q-switched pulses shown in Figure 21 are only instrumentation artifacts.

b. 10 Hz Q-switching

Both materials displayed the same pulse widths at 10 Hz as they did at 1 Hz for similar input energies. Figure 28 shows that the YAG was 35 ns for 10.6 J input and 45 ns for 13.3 J. The BEL pulse width remained near 100 ns for the same pump energies. Like the 1 Hz results this 100 ns pulse width was probably instrumentation broadened. Since 10 Hz operation led to coating damage, a repeated effort to measure narrower pulse widths for BEL was not attempted.

## SECTION V

### DISCUSSION AND CONCLUSIONS

Measurements indicated superior Q-switched efficiency for Nd:BEL, but better long pulse performance in Nd:YAG. This was demonstrated at 1 Hz and at 10 Hz. Higher Q-switched energy output was available with Nd:BEL probably because of its lower gain. This lower gain makes higher energy storage possible due to decreased parasitic effects such as amplified stimulated emission. If the higher energy can be swept out efficiently, (the slightly lower lifetime of Nd:BEL makes this more difficult), there is increased output.

For 1 Hz Q-switched operation, no change in slope efficiency was observed in the BEL rod up through an output energy of 350 mJ. Conversely, the YAG material approached an asymptote of 150 mJ output as input energy increased. At 10 Hz operation similar behavior was observed. The BEL showed no nonlinearity while the YAG output rolled off near 100 mJ. The slope efficiency recorded for Nd:YAG at 1 Hz long pulse operation was a near phenomenal 5.2%. Its advantage over the 3.4% value for Nd:BEL can be attributed to its greater upper laser level lifetime. Also surprising was BEL's 67% increase in efficiency when operated at 10 Hz. A possible explanation may be more even thermal loading at the increased repetition rate.

Beam divergence data showed that the X-axis cut Nd:BEL rod performed comparably to the Nd:YAG rod in the area of thermal lensing. As was to be expected, the BEL output was more elliptical because of its birefringent nature. However, the calculated divergence values showed BEL to be superior at 10 Hz Q-switched operation, roughly equal at 1 Hz Q-switched, and superior at 1 Hz long pulse. The oscillatory nature of the divergence displayed by both materials was interesting. Under stable resonator

conditions, one would expect the thermal lensing to increase with increasing input energy. Decrease of divergence at higher input energies may mean the laser cavity was passing in and out of unstable resonator configurations.

The Nd:YAG and Nd:BEL rods showed similar pulse to pulse stability. Casual observation of the energy readings during the  $E_{in}$  vs  $E_{out}$  measurements support the data taken with the X-Y recorder. Of all the measurements obtained, the most improvement could be made in the pulse shape area. Accurate temporal shapes were not obtainable with the equipment available and would have been very useful.

The fact that BEL's pulse width was substantially larger than YAG's and that YAG's increased with increased pump energy was not to be expected. An inaccurate cut of the BEL rod may cause polarization alignment problems for the Q-switch and widen the pulse width, but it is unlikely that it would have that much of an effect. Increasing pulse widths for increasing energy may be partially explained by saturation of the detection system, but this is also unlikely. Therefore the measurement was repeated for BEL at 1 Hz Q-switching. The result showed a pulse width that was comparable to YAG.

Nd:BEL has potential for use in military applications, especially in the area of Q-switched pulsed output. Its natural polarization offers advantages and its comparable threshold to YAG make it practical from an efficiency standpoint. Because of the need for multifunction optical sources, an evaluation of high rep rate and high average power performance needs to be conducted. The material will also have to provide low divergence beam shapes for high power applications.

## REFERENCES

1. J. Ceusic, H. Marcos, L. Uitert, "Laser Oscillations in Nd-doped Yttrium Aluminum, Yttrium Gallium and Gadolinium Garnets", *Applied Physics Letters*, Vol. 4, No. 10.
2. N. Barnes, D. Gettemy, Comparison of Nd 1.06 and 1.33  $\mu\text{m}$  Operation in Various Hosts, Los Alamos National Laboratory, May 1986.
3. E. Reed, "A Flashlamp-Pumped, Q-switched Cr:Nd:GSGG Laser", *IEEE Journal of Quantum Electronics*, Vol. QE-21, No. 10, Oct 1985.
4. T. Pollak, W. Wing, R. Grasso, E. Chicklis, and H. Jenssen, "CW Laser Operation of Nd:YLF", *IEEE Journal of Quantum Electronics*, Vol. QE-18, No. 2, Feb 1982.
5. S. Singh, R. Smith, L. Van Uitert, "Stimulated emission cross section and fluorescent quantum efficiency of Nd<sup>3+</sup> in yttrium aluminum garnet at room temperature", *Physical Review B*, Vol. 10, No. 6, Sep 1974.
6. R. Morris, C. Cline, R. Begley, M. Dutoit, P.J. Harget, H. Jenssen, T.S. LaFrance, and R. Webb, "Lanthanum Beryllate: A new rare-earth ion laser host", *Applied Physics Letters*, Vol. 27, No. 8, 1975.
7. H. Jenssen, R. Begley, R. Webb, and R.G. Moore, "Spectroscopic properties and laser performance of Nd<sup>3+</sup> in lanthanum beryllate", *Journal of Applied Physics*, Vol. 47, NO. 4, April 1976.
8. Handbook of Laser Science and Technology, Vol. I, M. Weber, editor, CRC Press, Boca Raton, Fla., 1982.

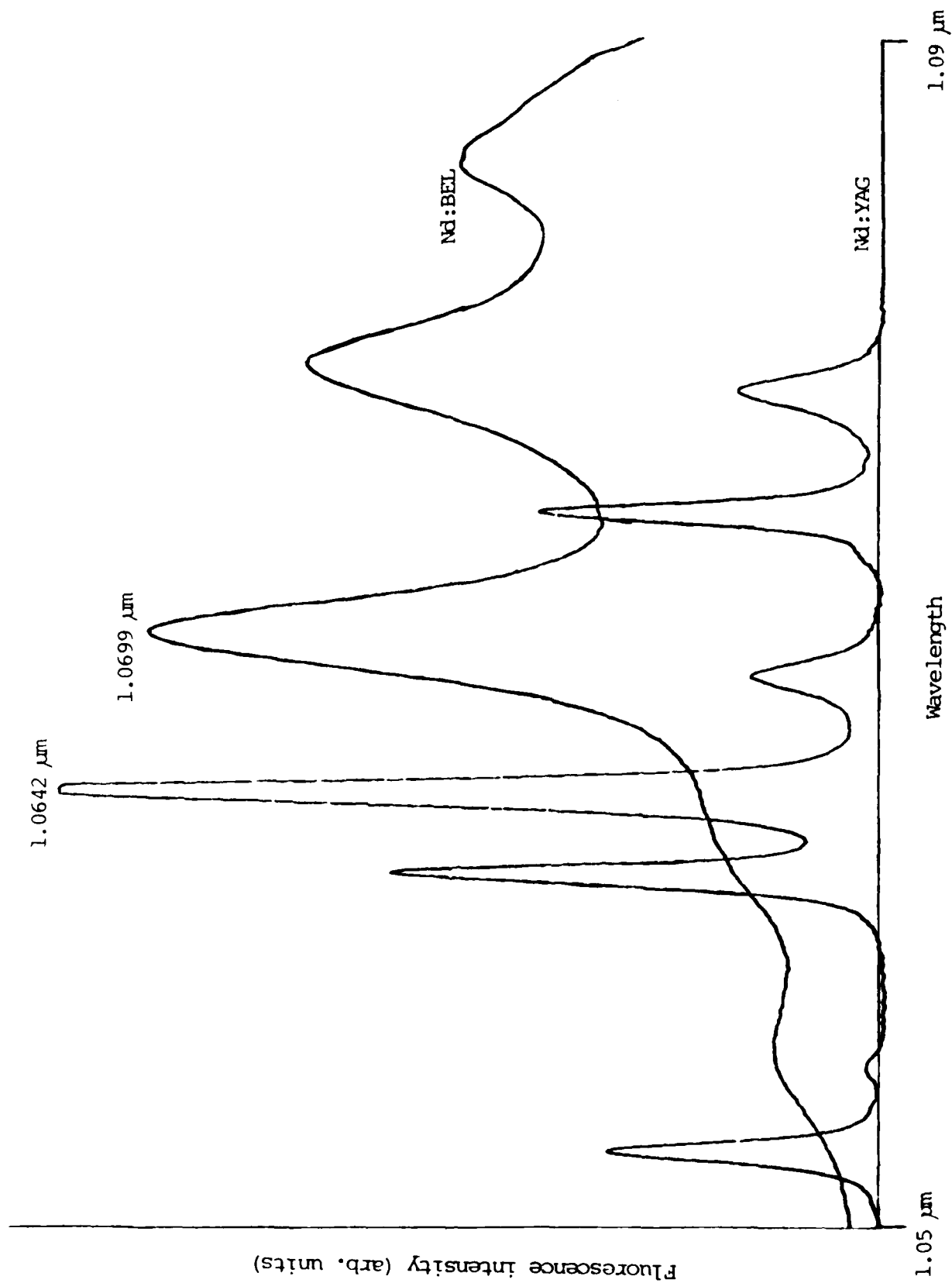


Figure 1 - Fluorescence Spectra of Nd:BEL and Nd:YAG rods

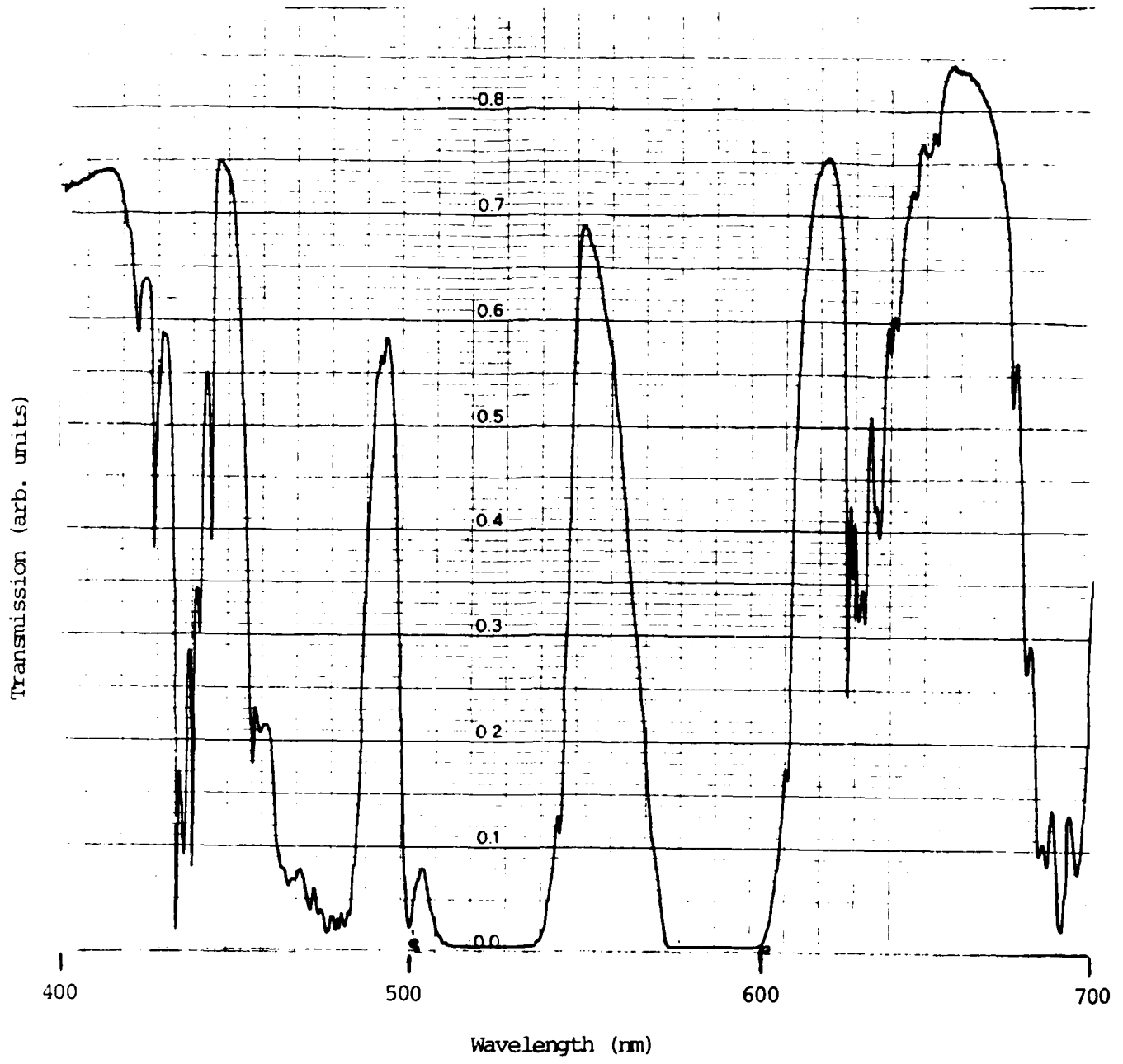


Figure 2 - Absorption Spectrum of Nd:BEL laser rod

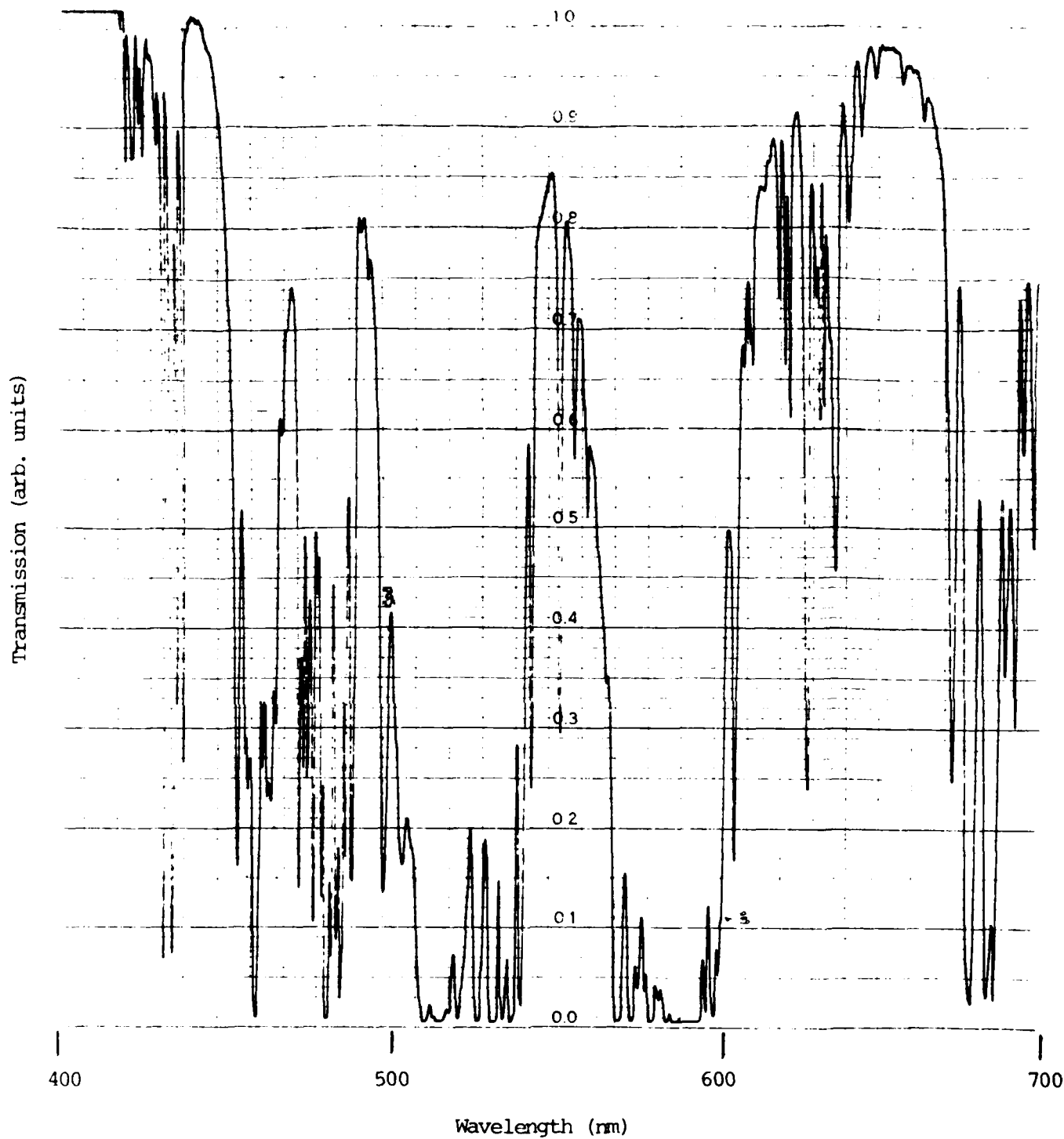


Figure 3 - Absorption Spectrum of Nd:YAG laser rod

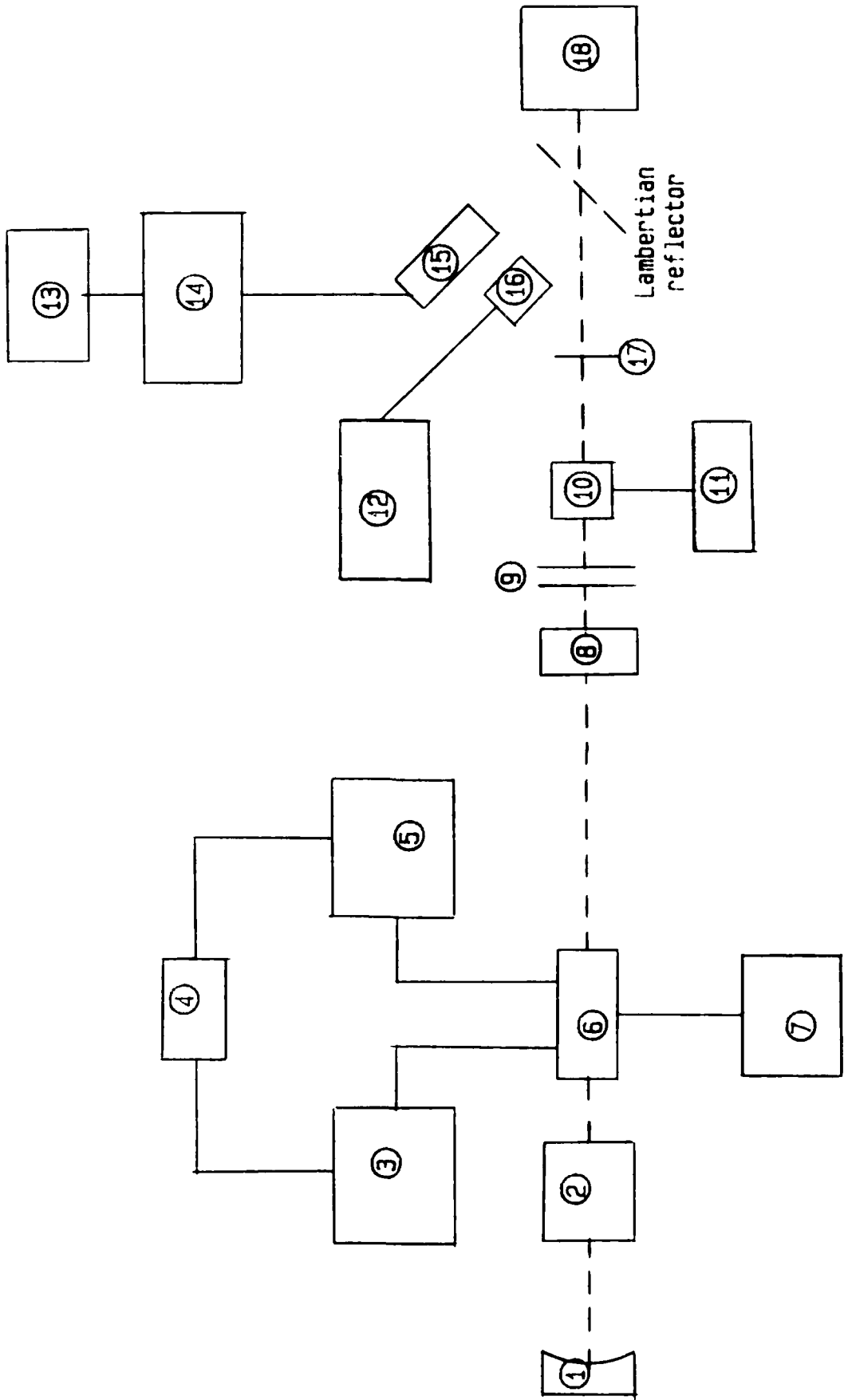
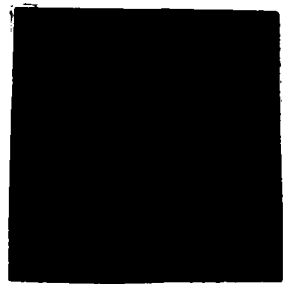


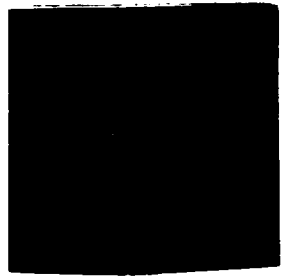
Figure 4 - Schematic of Laboratory Set Up



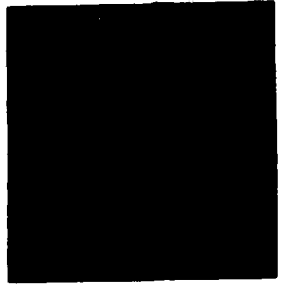
100 cm.



150 cm.



200 cm.



250 cm.

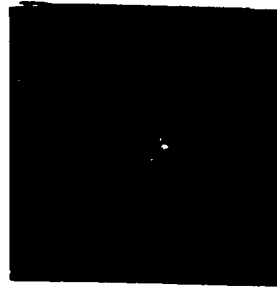
1 Hz Q-switched Nd:YAG



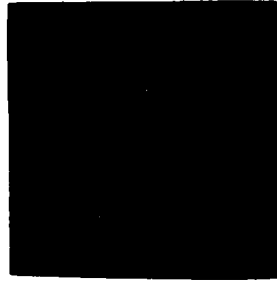
100 cm.



150 cm.



200 cm.



250 cm.

1 Hz Q-switched Nd:BEL

Figure 5 - Spot Images of Laser Output (Varying distances from output mirror)

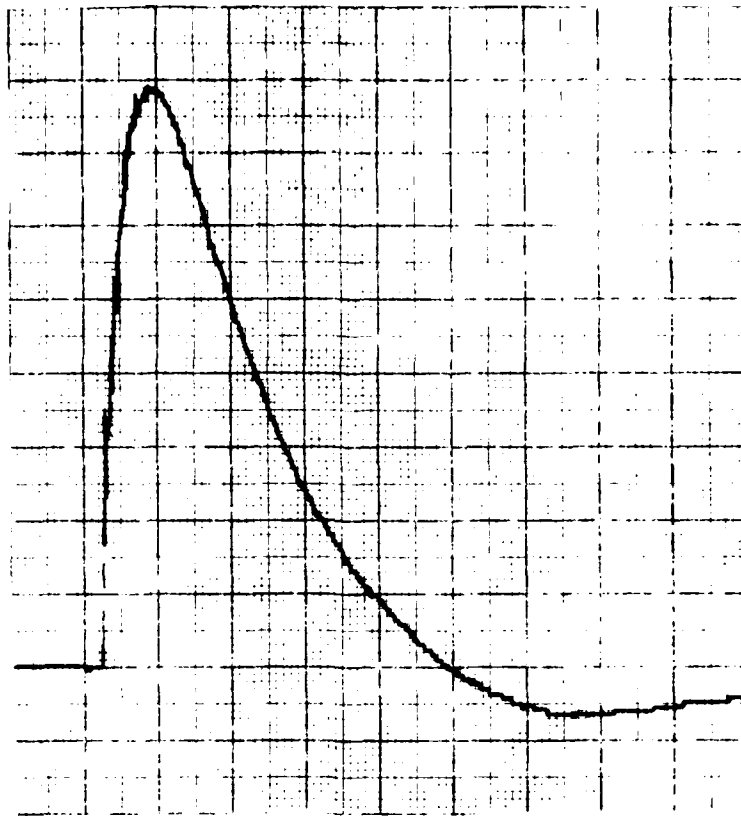


Fig. 6a 1 Hz Long Pulse Nd:YAG at 24.5 J Pumping

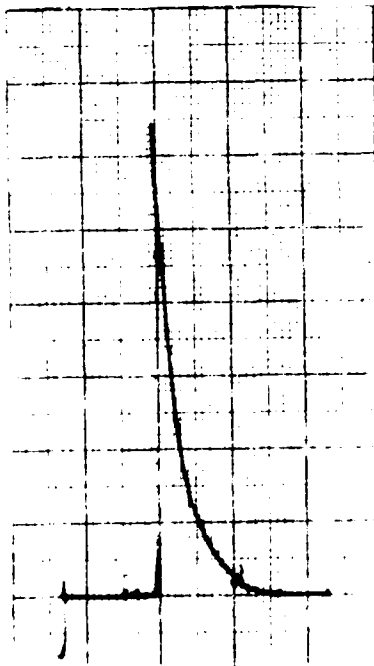


Fig. 6b 1 Hz Q-switched Nd:BEL  
at 14 J Pumping

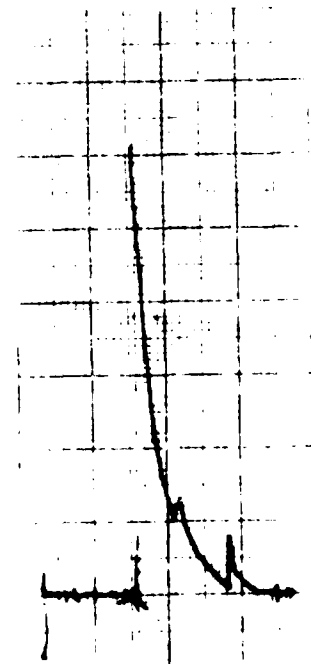


Fig. 6c 1 Hz Q-switched Nd:BEL  
at 17 J Pumping

Figure 6 - Pulse to Pulse Stability Recordings

# Long Pulse Lasing of Nd:YAG at 1 Hz

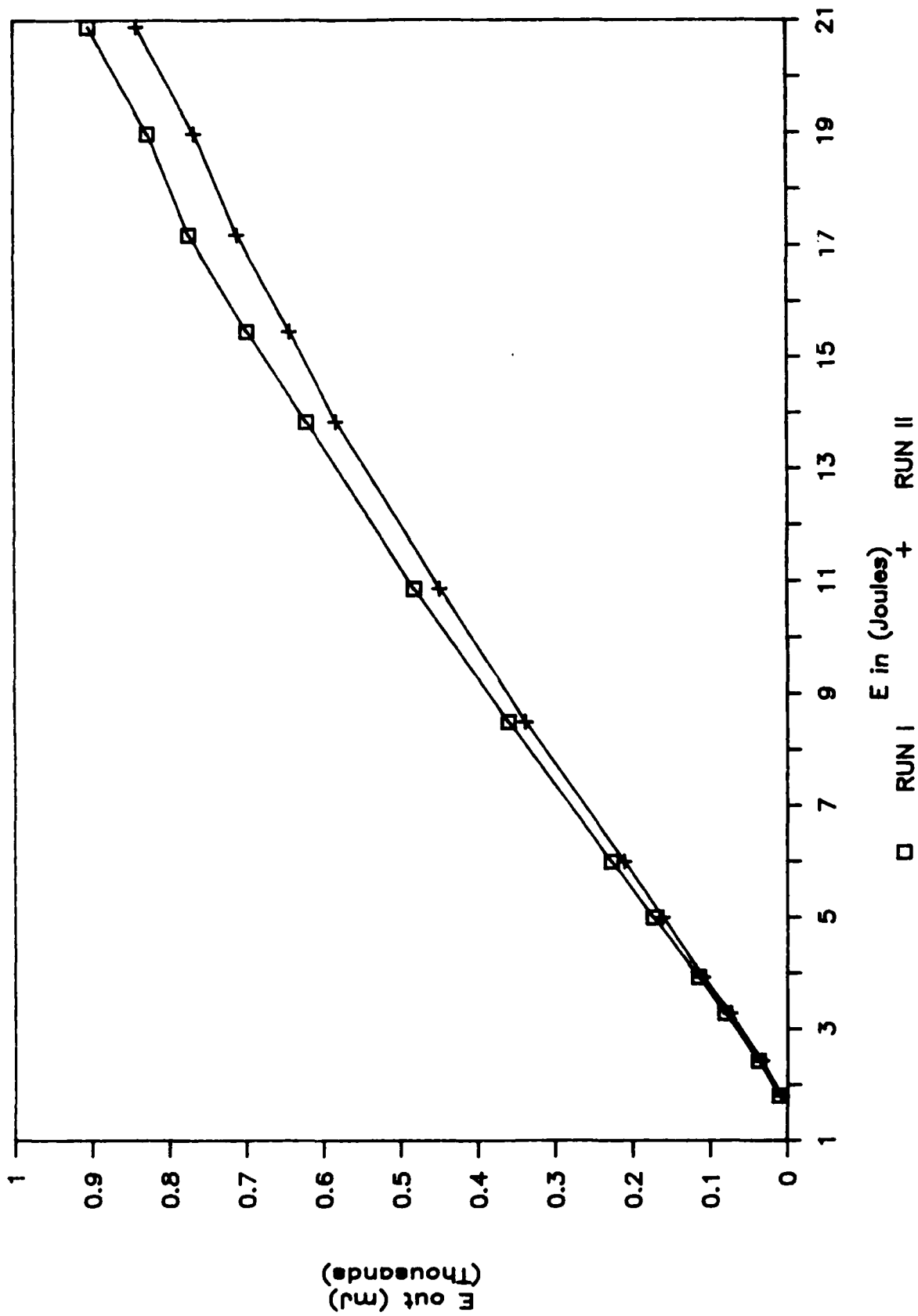


Figure 7 -  $E_{in}$  vs  $E_{out}$  for Long Pulse Nd:YAG at 1 Hz

# Long Pulse Lasing Comparison at 1 Hz

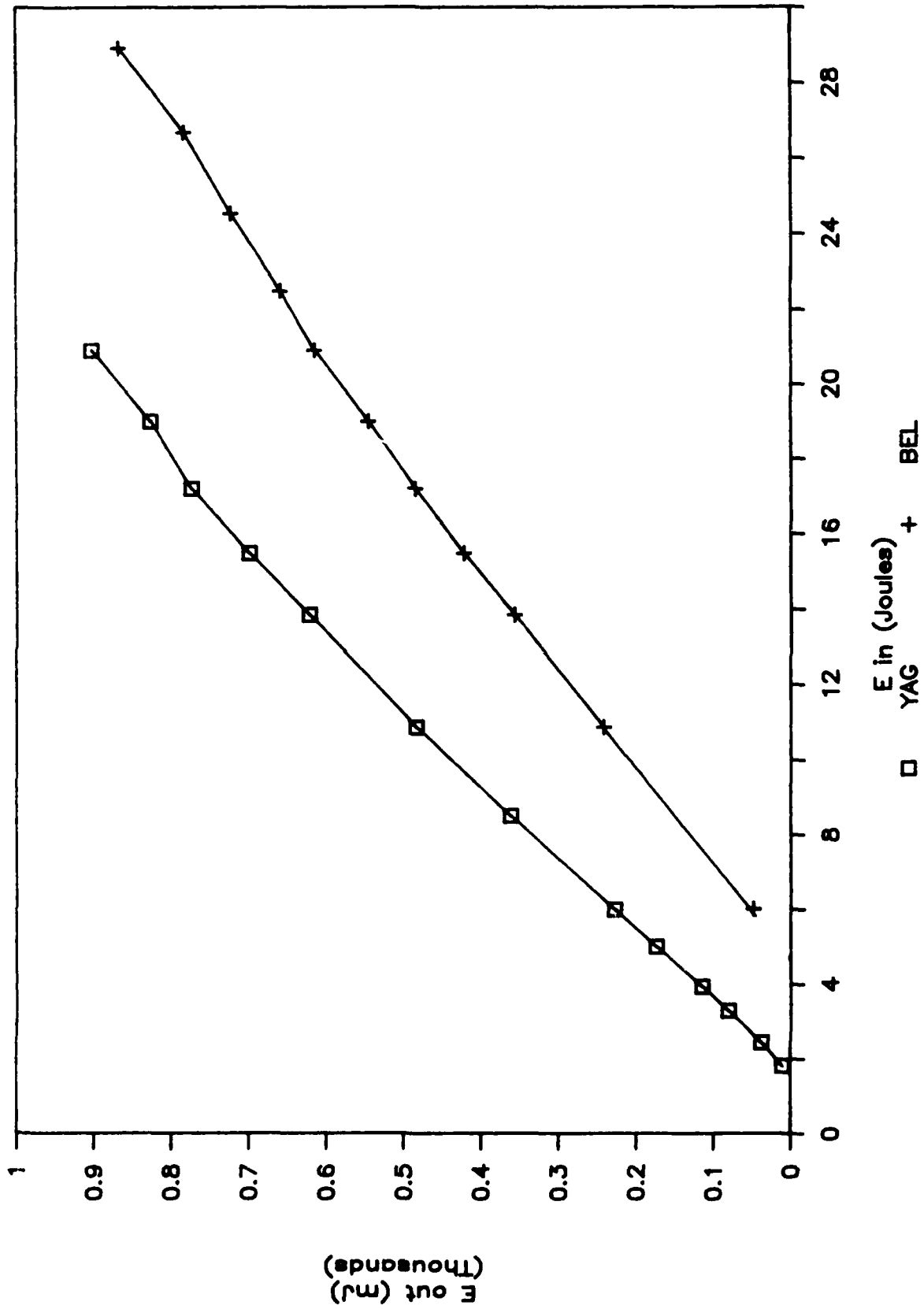


Figure 8 -  $E_{in}$  vs  $E_{out}$  for Long Pulse Nd:YAG and Nd:BEL at 1 Hz

Long Pulse Lasing of Nd:BEL at 1.08  $\mu\text{m}$   
(polarizer in cavity)

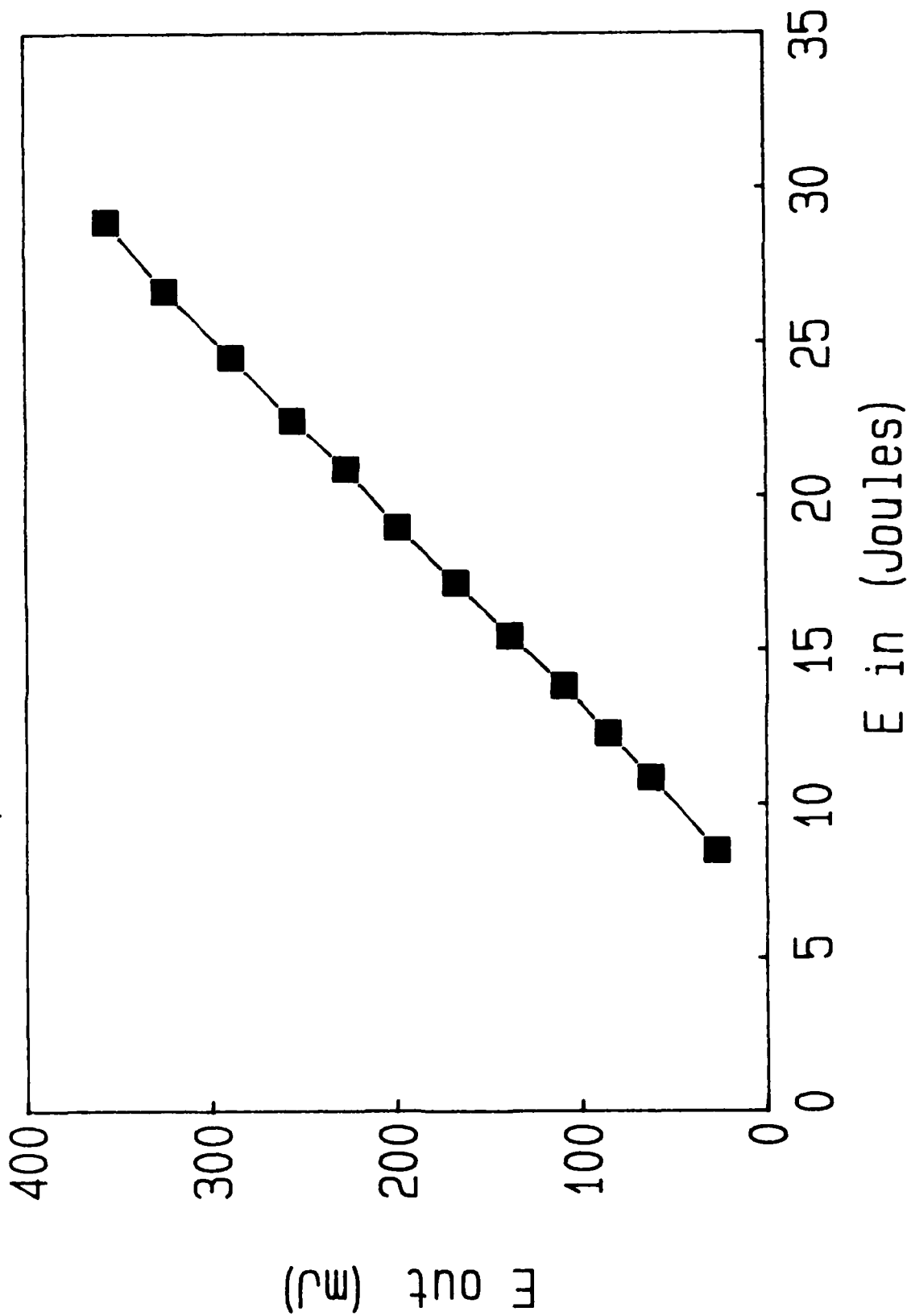


Figure 9 -  $E_{in}$  vs  $E_{out}$  for 1.08  $\mu\text{m}$  Nd:BEL at 1 Hz

Long Pulse Lasing of Nd:BEL at 1.07  $\mu\text{m}$   
(polarizer in cavity)

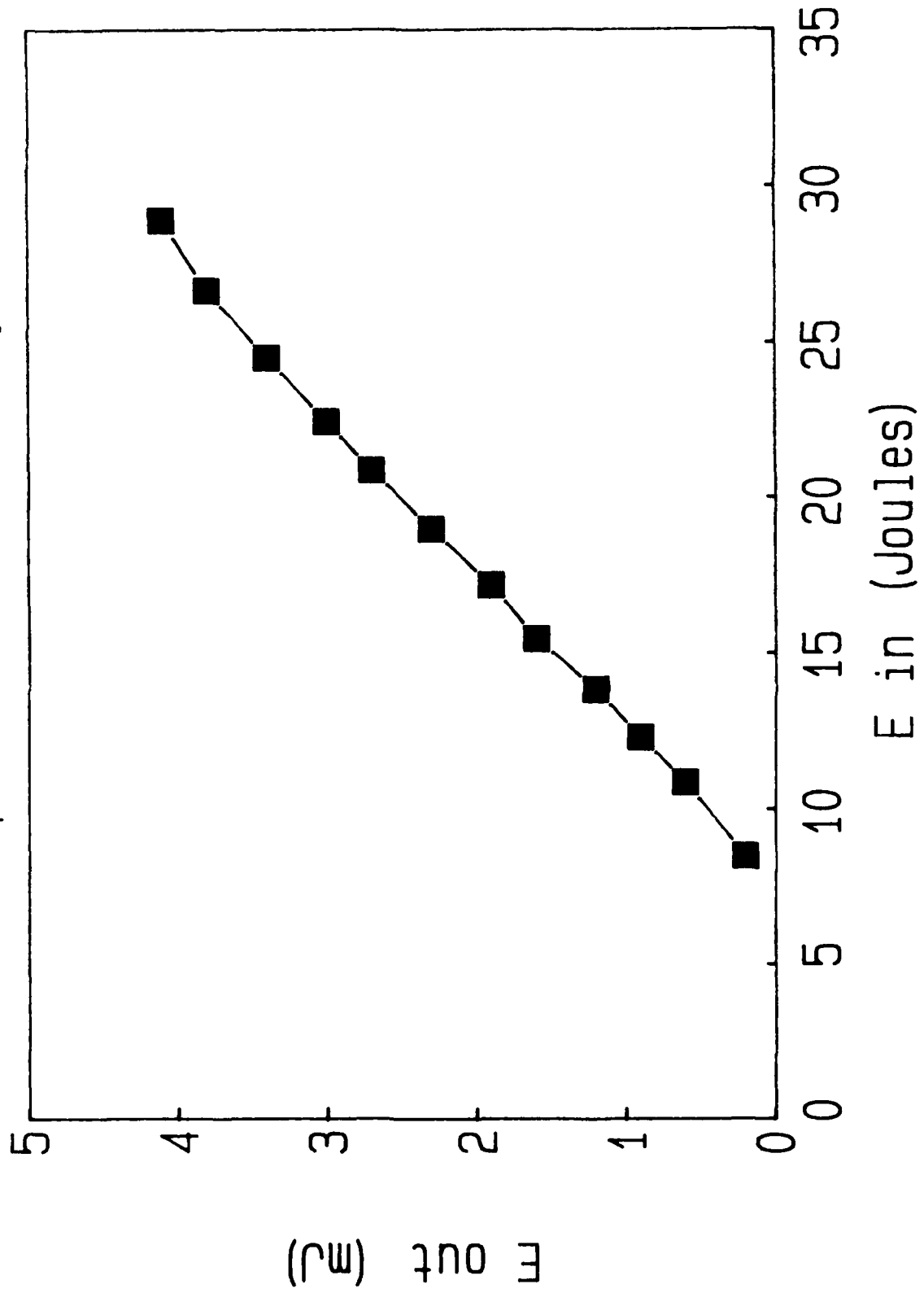


Figure 10 -  $E_{in}$  vs  $E_{out}$  for 1.07  $\mu\text{m}$  Nd:BEL at 1 Hz

# Long Pulse Lasing Comparison at 10 Hz

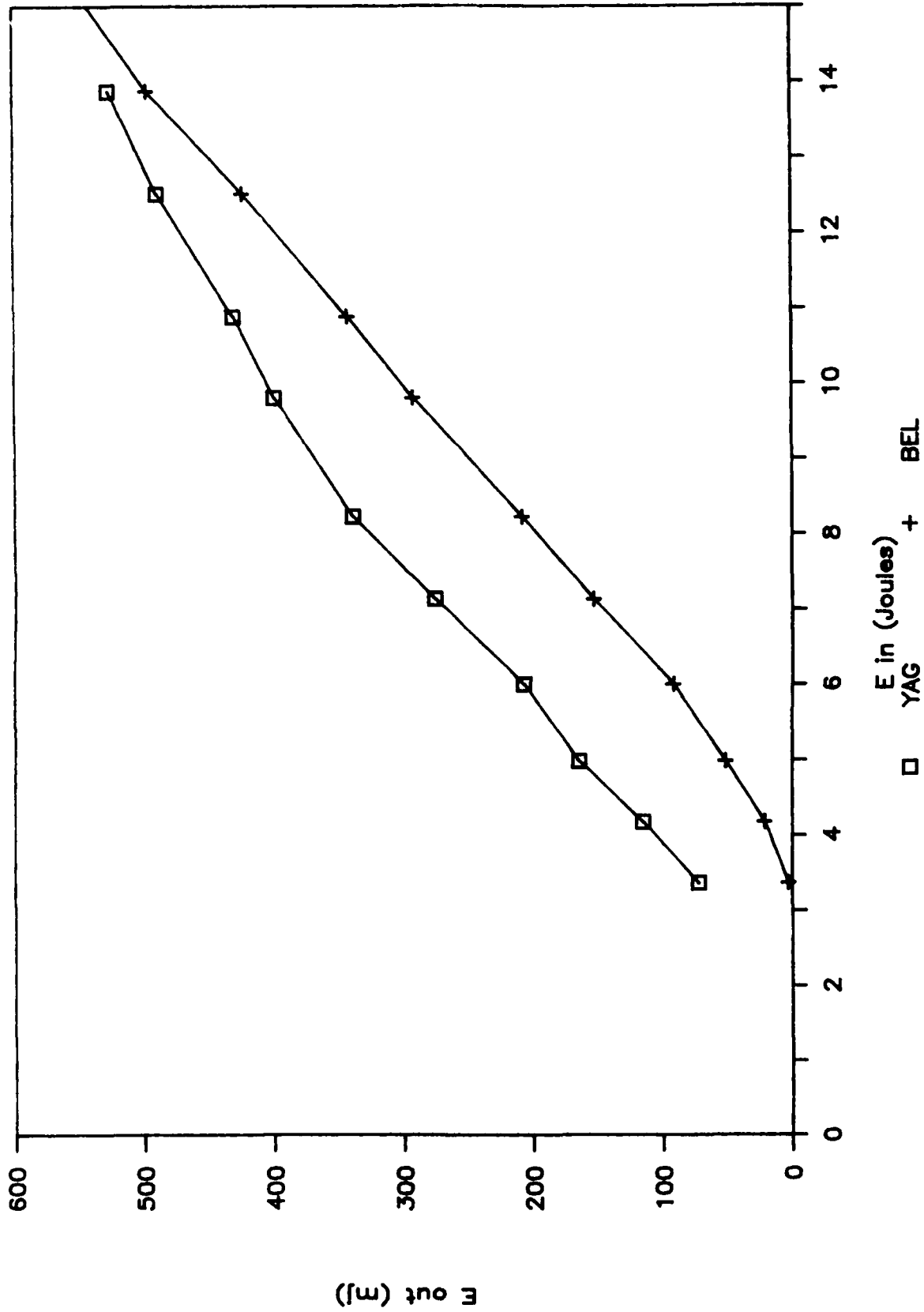


Figure 11 -  $E_{in}$  vs  $E_{out}$  for Long Pulse Nd:YAG and Nd:BEL at 10 Hz

# Q-switched Lasing Comparison at 1 Hz

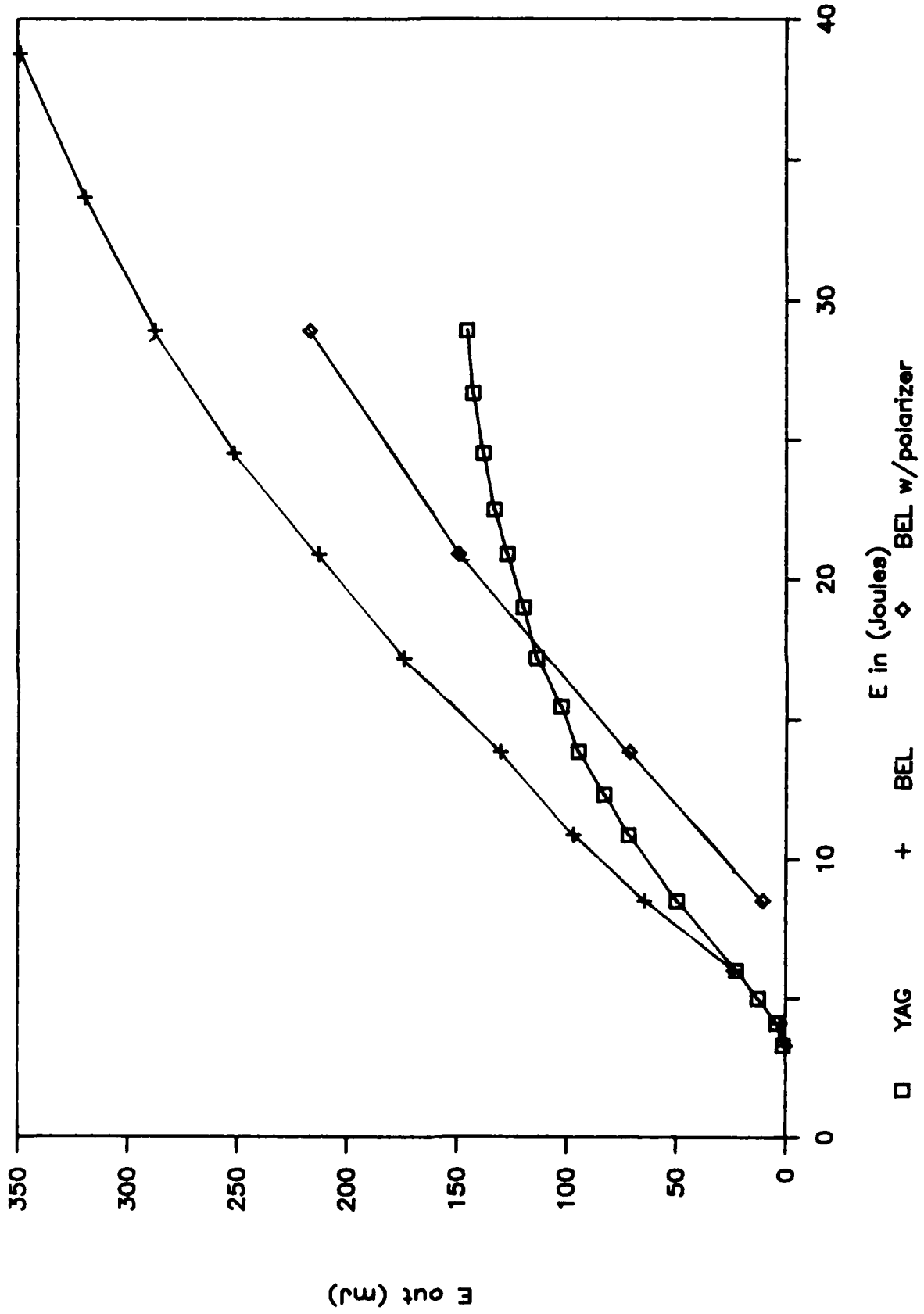


Figure 12 - E<sub>in</sub> vs E<sub>out</sub> for Q-switched Nd:YAG and Nd:BEL at 1 Hz

# Q-switched Lasing Comparison at 10 Hz

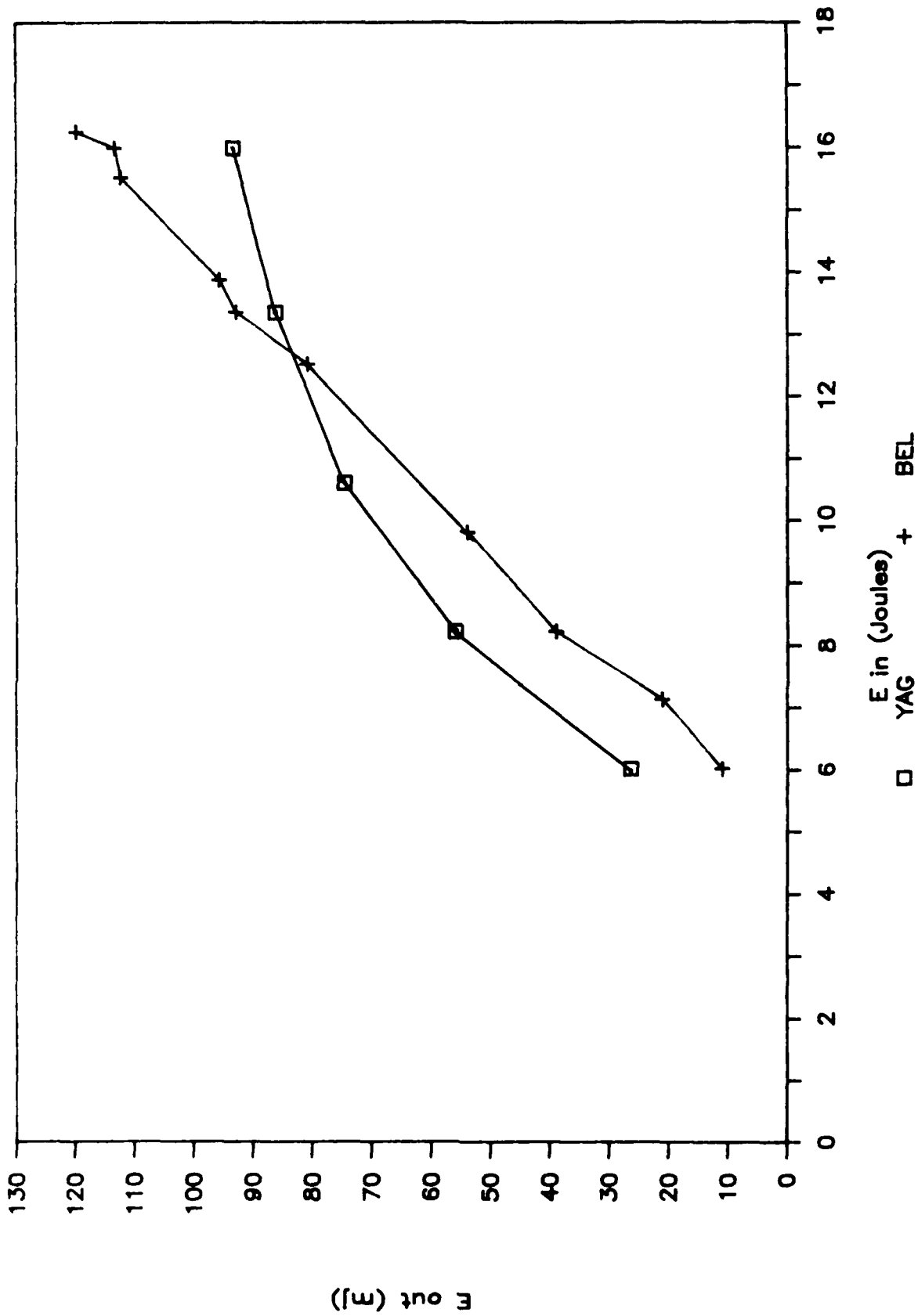


Figure 13 -  $E_{in}$  vs  $E_{out}$  for Q-switched Nd:YAG and Nd:BEL at 10 Hz

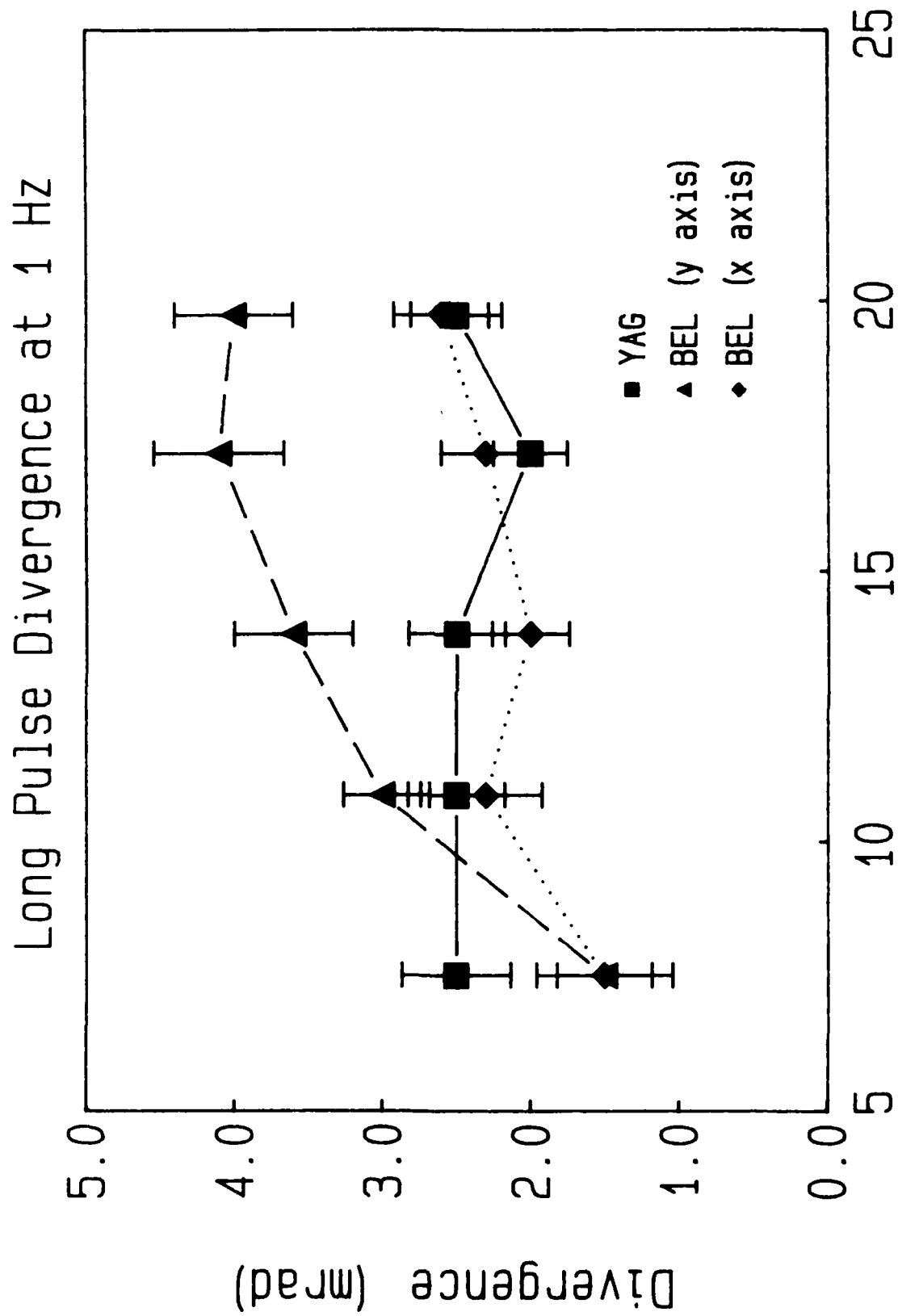


Figure 14 - Long Pulse Beam Divergence

# Q-switched Divergence at 1 Hz

X axis

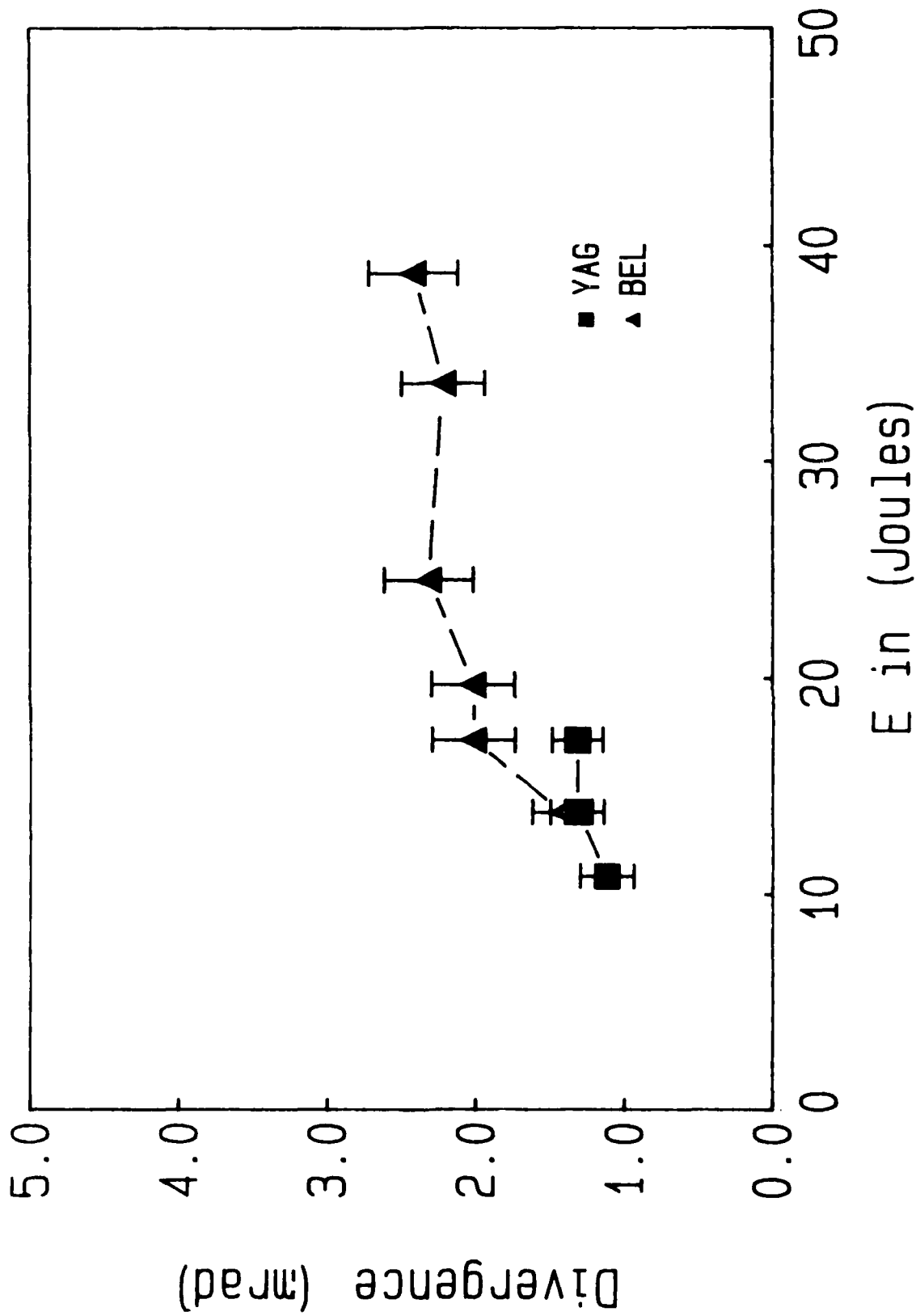
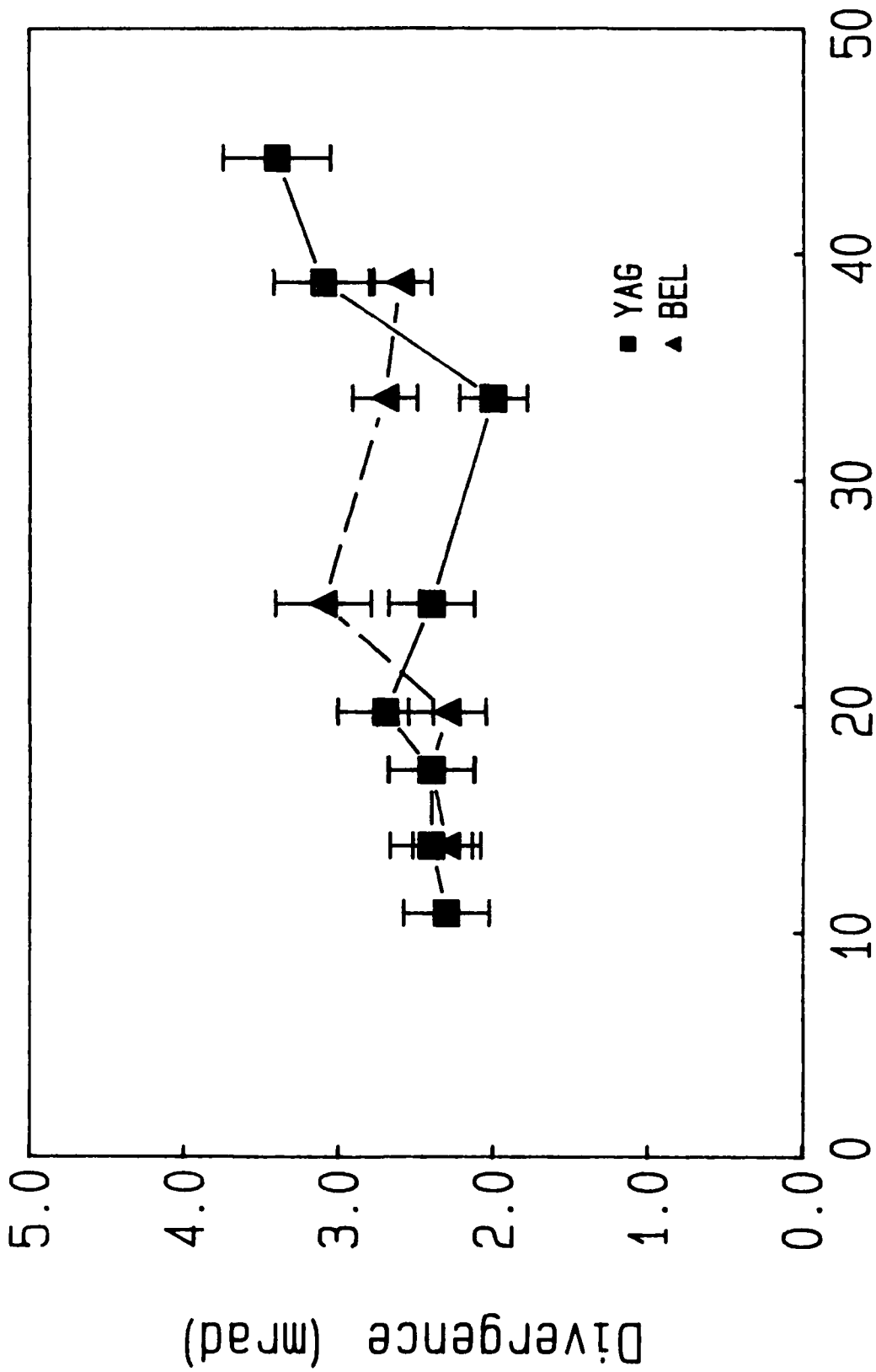


Figure 15 - 1 Hz Q-switched X axis Beam Divergence

# Q-switched Divergence at 1 Hz

Y axis



E in (Joules)

Figure 16 - 1 Hz Q-switched Y axis Beam Divergence

# Q-switched Divergence at 10 Hz X axis

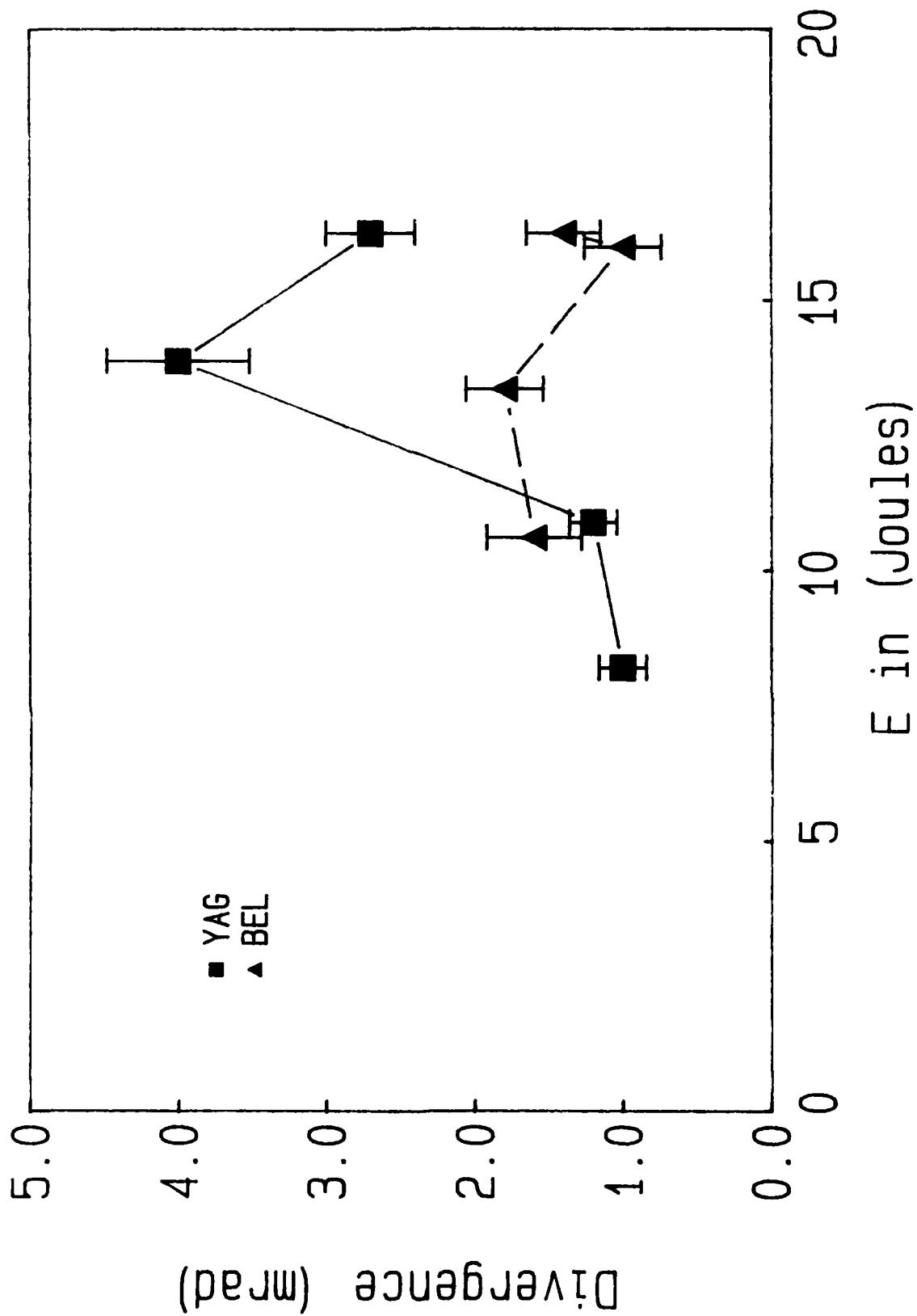


Figure 17 - 10 Hz Q-switched X axis Beam Divergence

# Q-switched Divergence at 10 Hz

Y axis

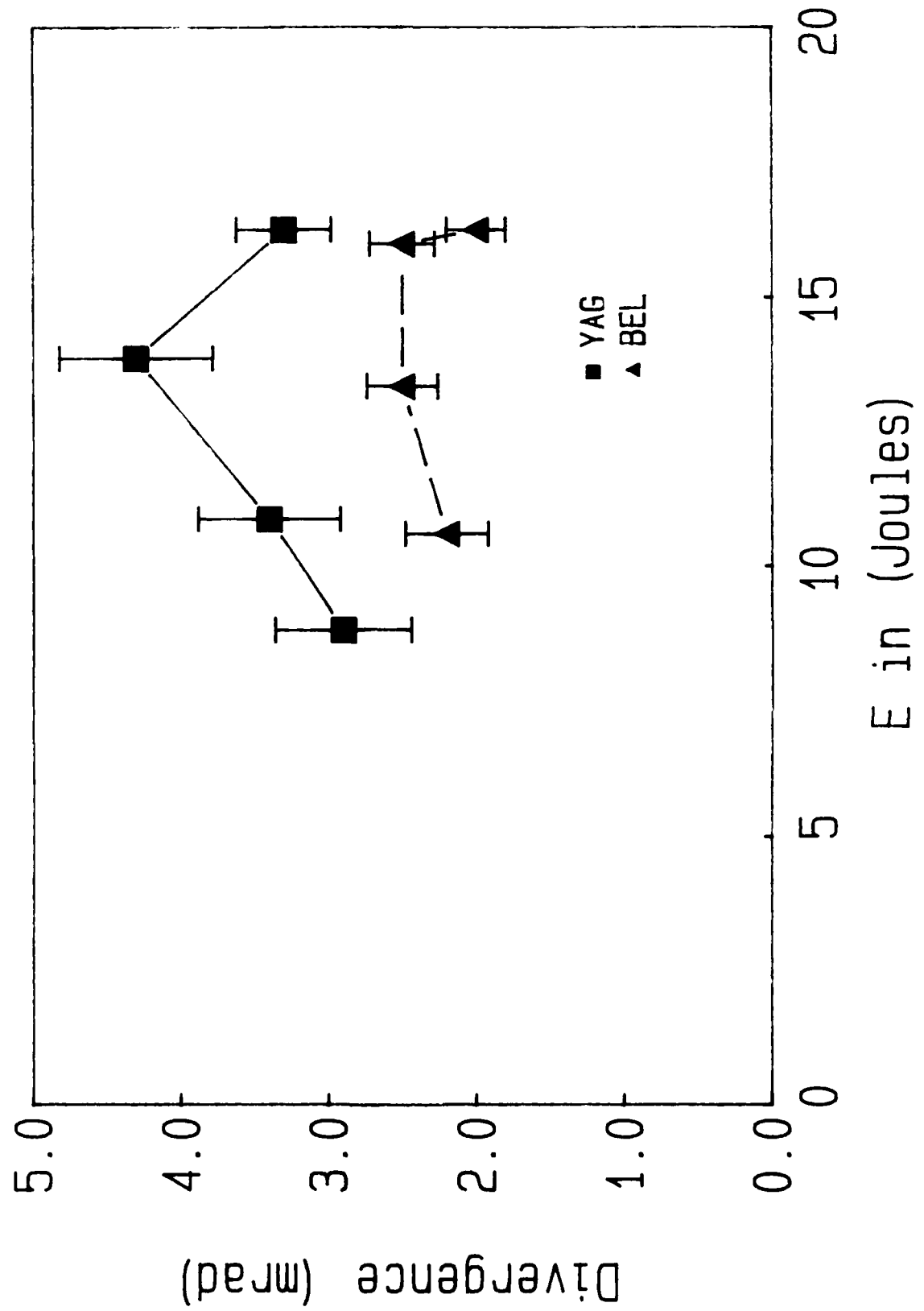


Figure 18 - 10 Hz Q-switched Y axis Beam Divergence

Nd: BEL

# 1 Hz Long Pulse Pulse to Pulse Stability

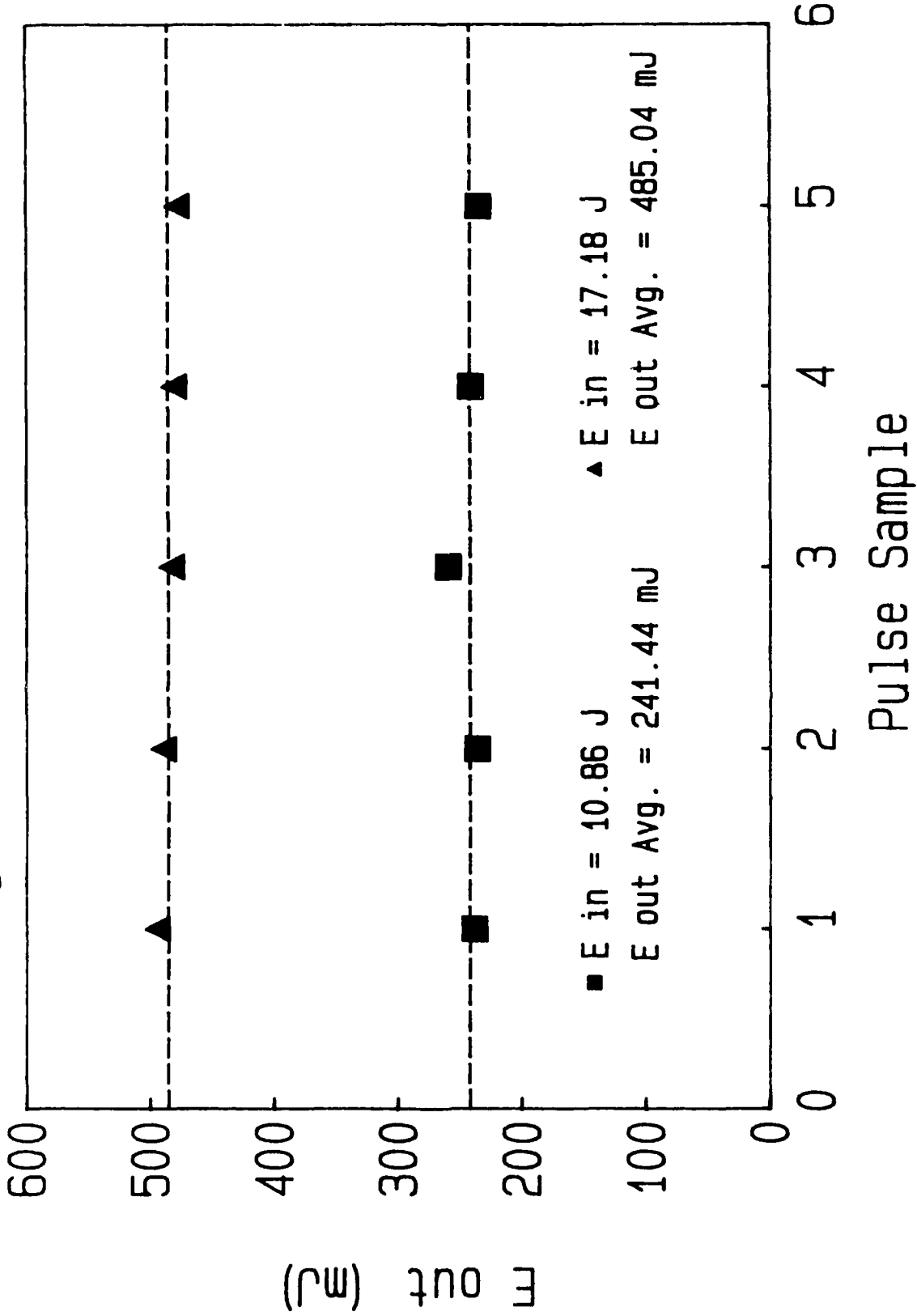


Figure 19 - Pulse to Pulse Stability for Long Pulse Nd:BEL at 1 Hz

Nd: YAG

1 Hz Long Pulse Pulse to Pulse Stability

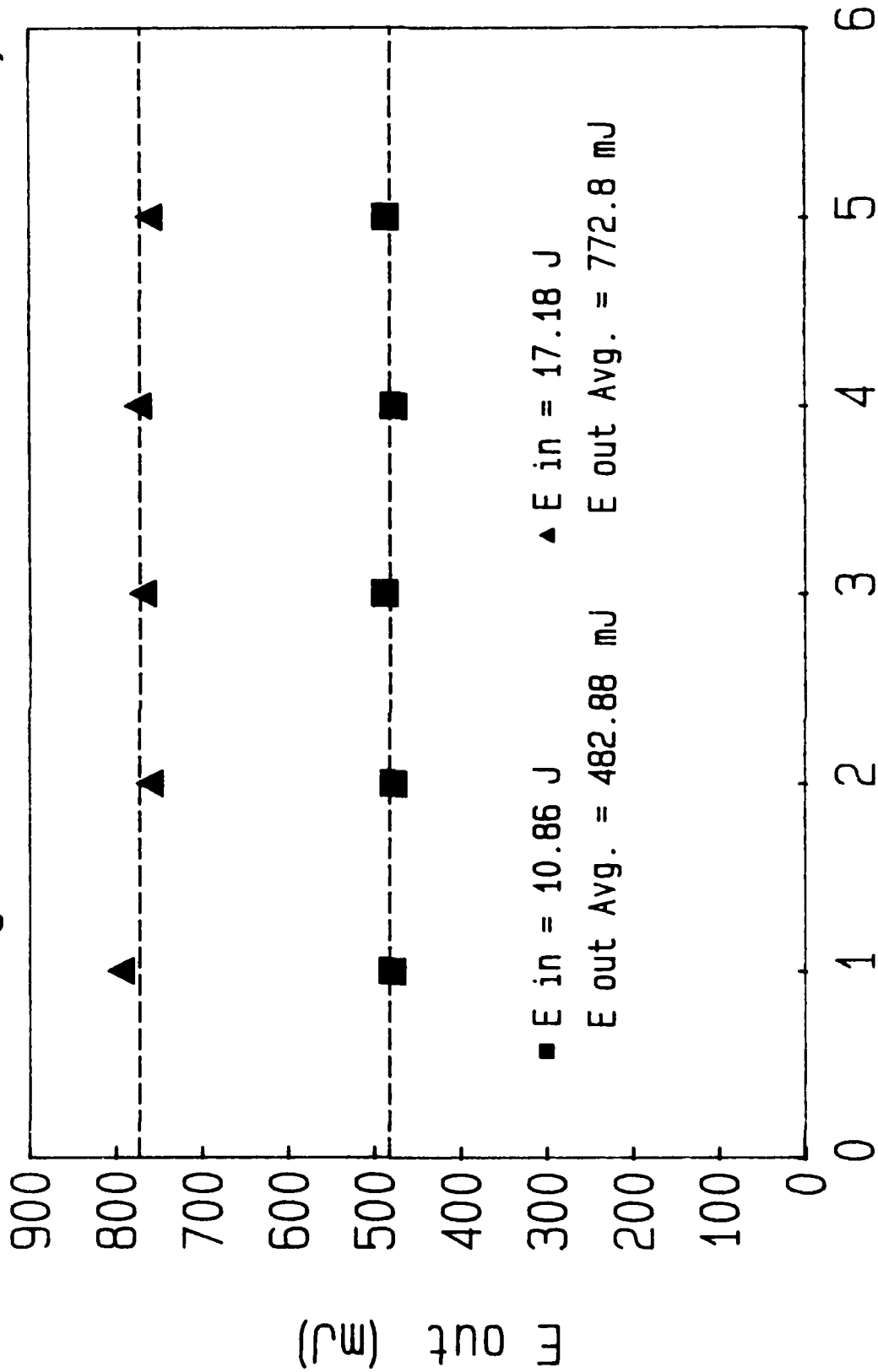
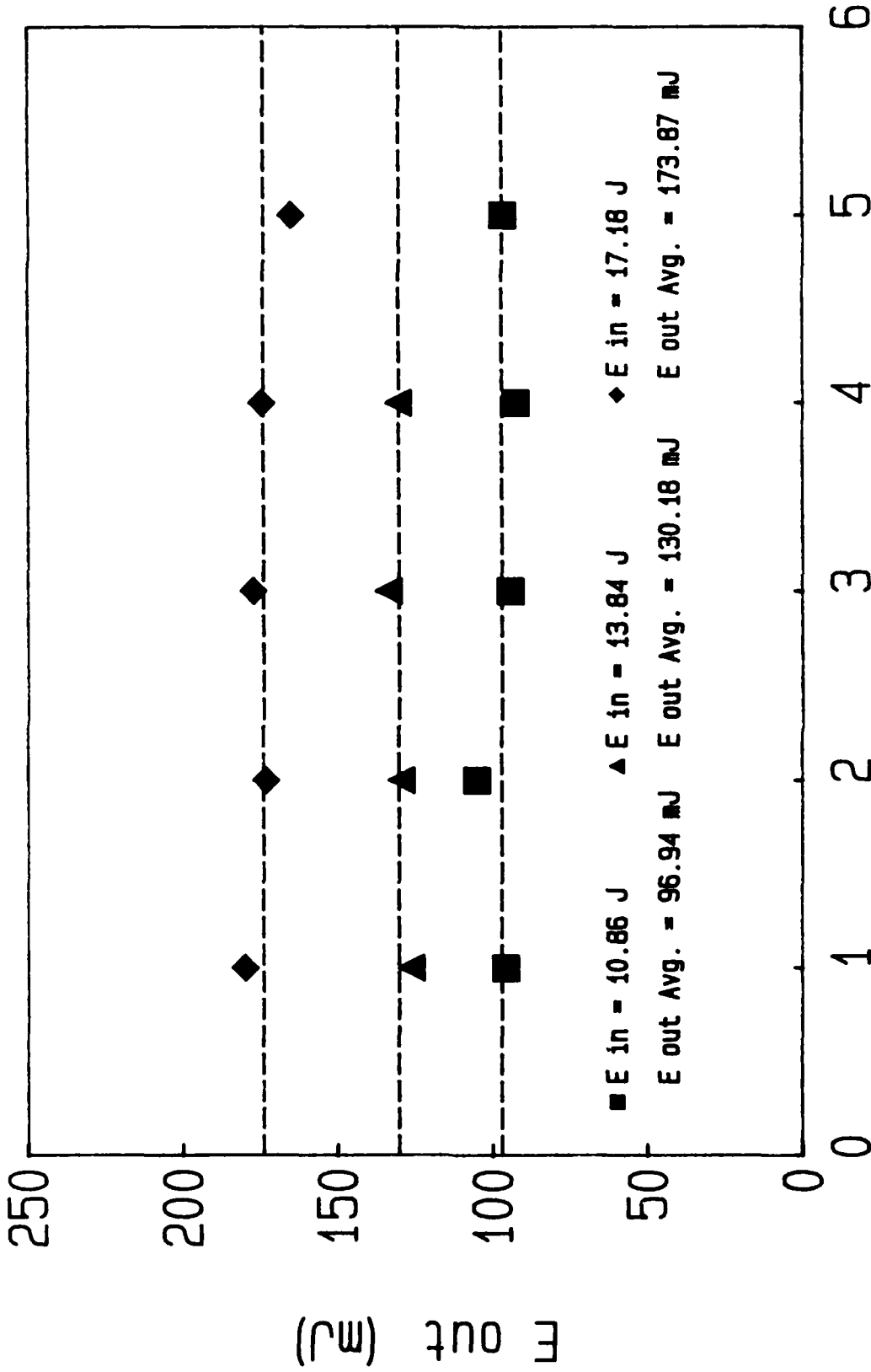


Figure 20 - Pulse to Pulse Stability for Long Pulse Nd:YAG at 1 Hz

Nd: BEL

1 Hz Q-switched Pulse to Pulse Stability



Pulse Sample

Figure 21 - Pulse to Pulse Stability for Q-switched Nd:BEL at 1 Hz

Nd: YAG

# 1 Hz Q-switched Pulse to Pulse Stability

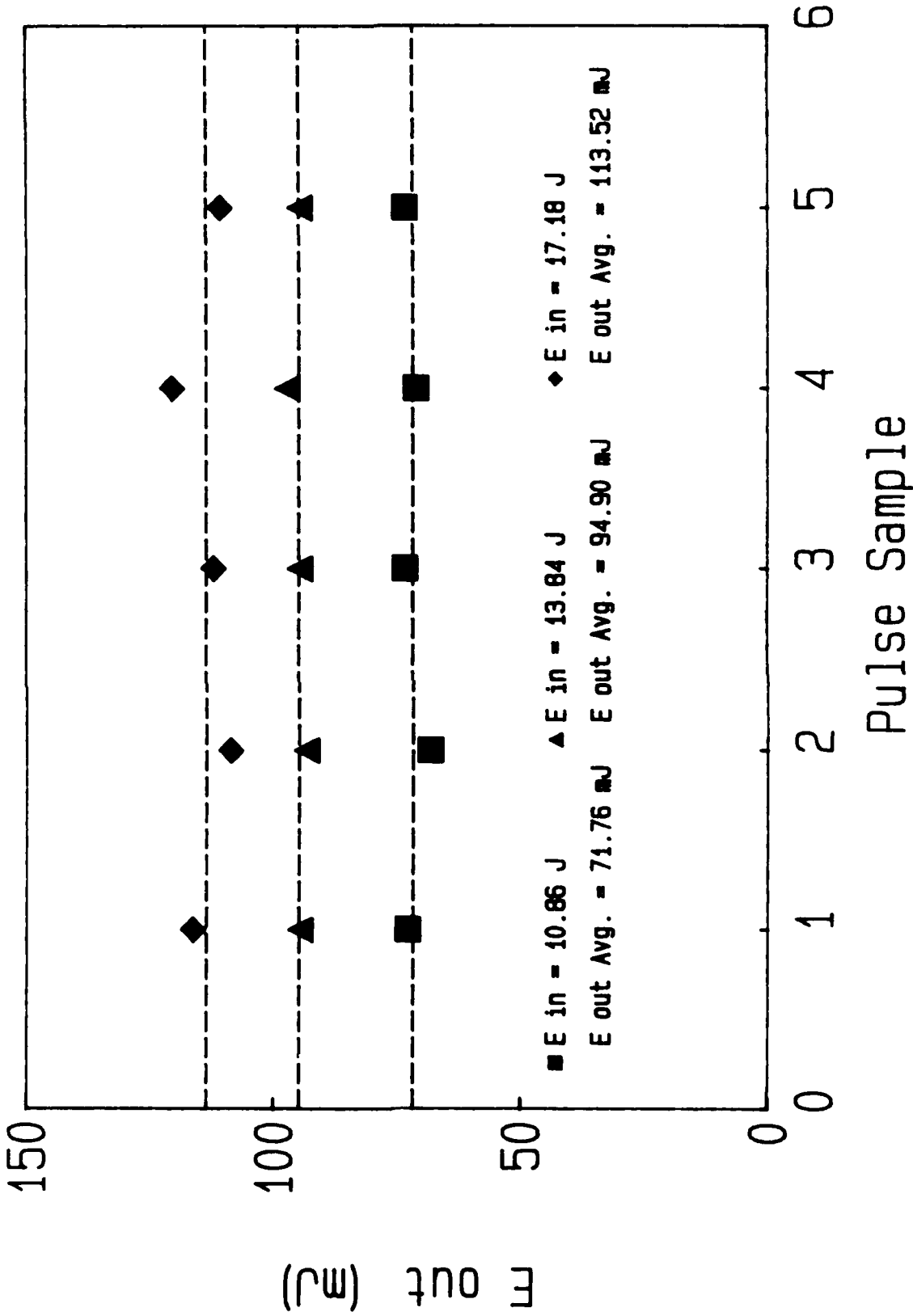


Figure 22 - Pulse to Pulse Stability for Q-switched Nd:YAG at 1 Hz

Nd:BEL

# 10 Hz Q-switched Pulse to Pulse Stability

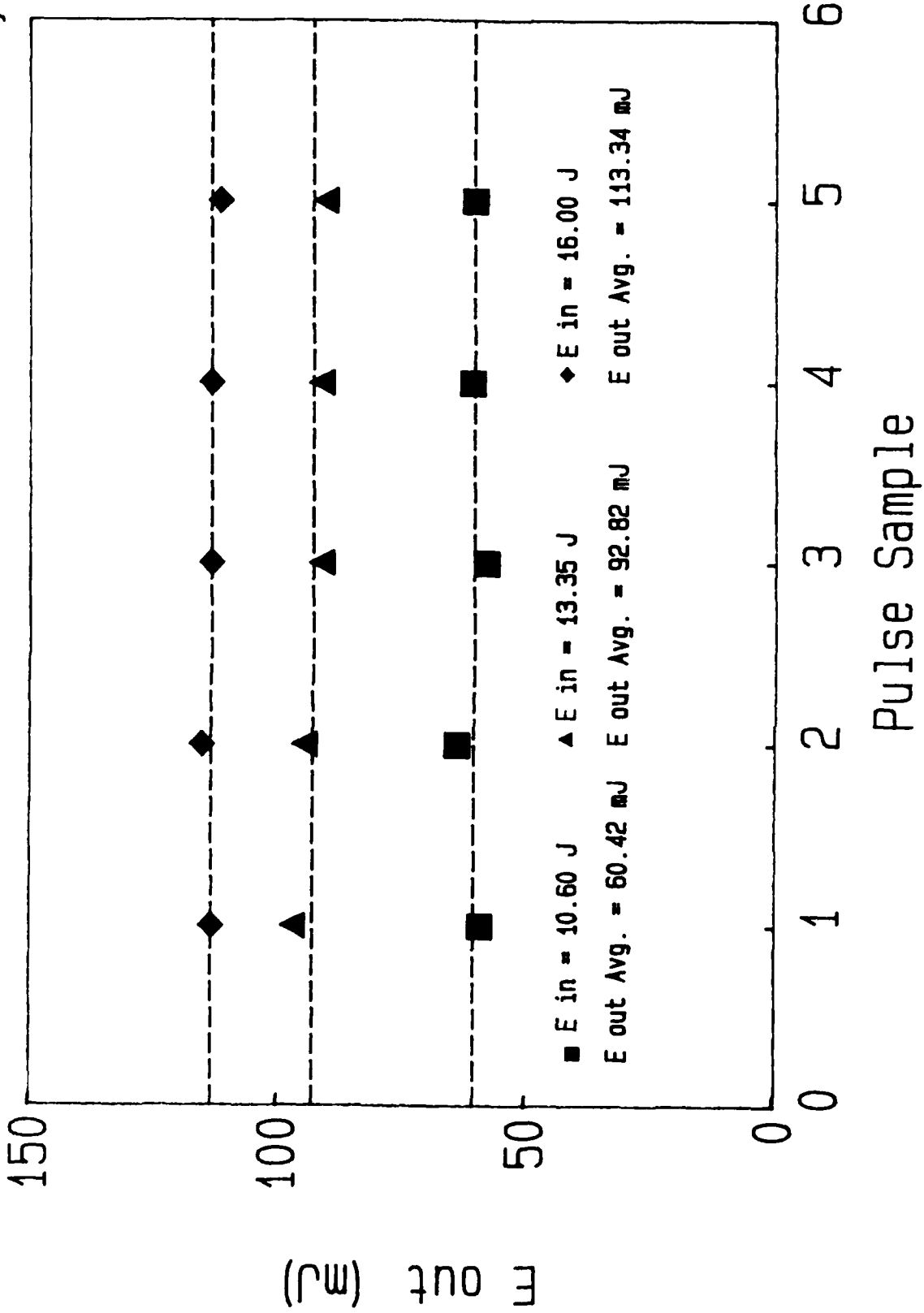


Figure 23 - Pulse to Pulse Stability for Q-switched Nd:BEL at 10 Hz

Nd: YAG

# 10 Hz Q-switched Pulse to Pulse Stability

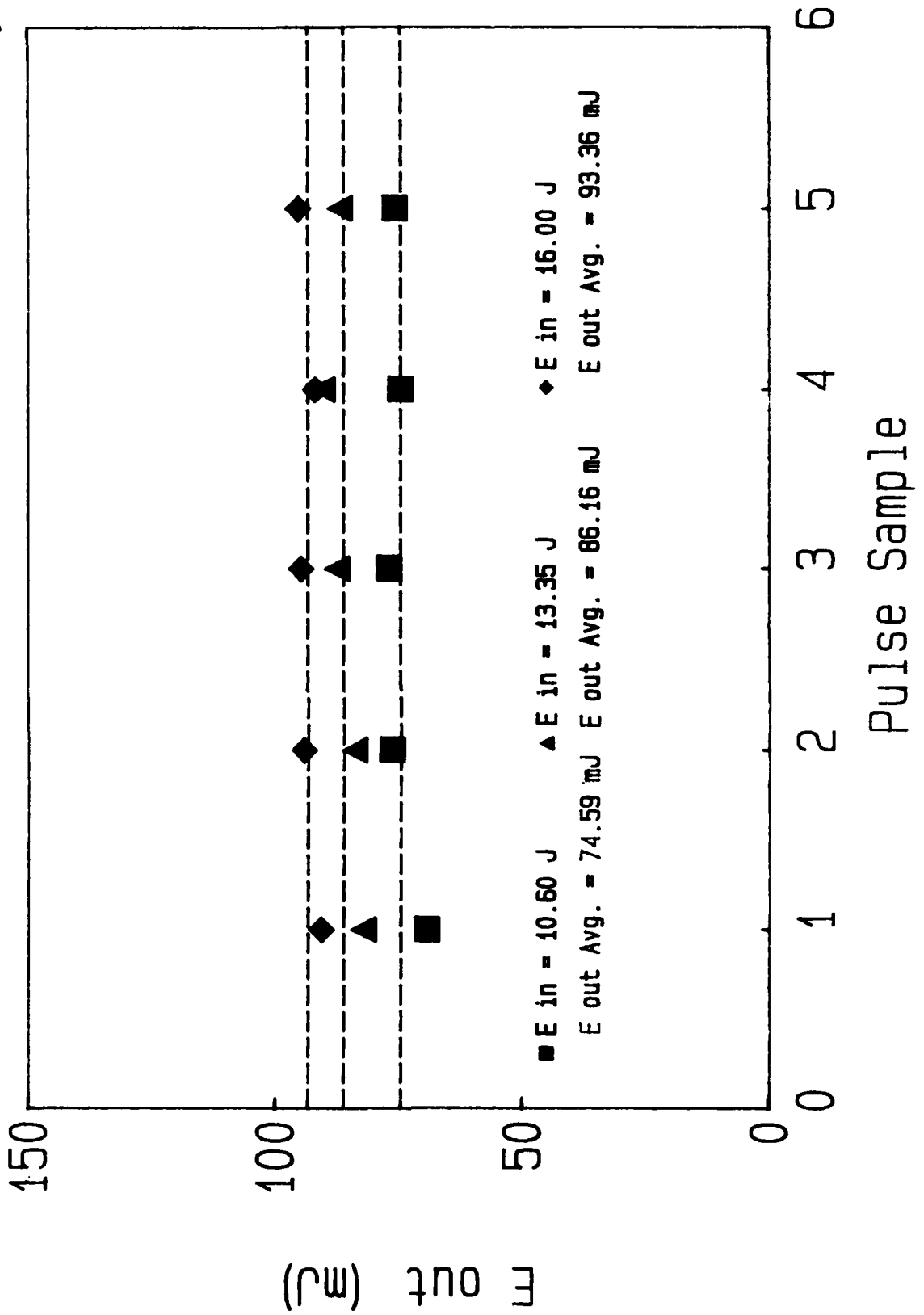


Figure 24 - Pulse to Pulse Stability for Q-switched Nd:YAG at 10 Hz

# Maximum to Minimum Energy Variations

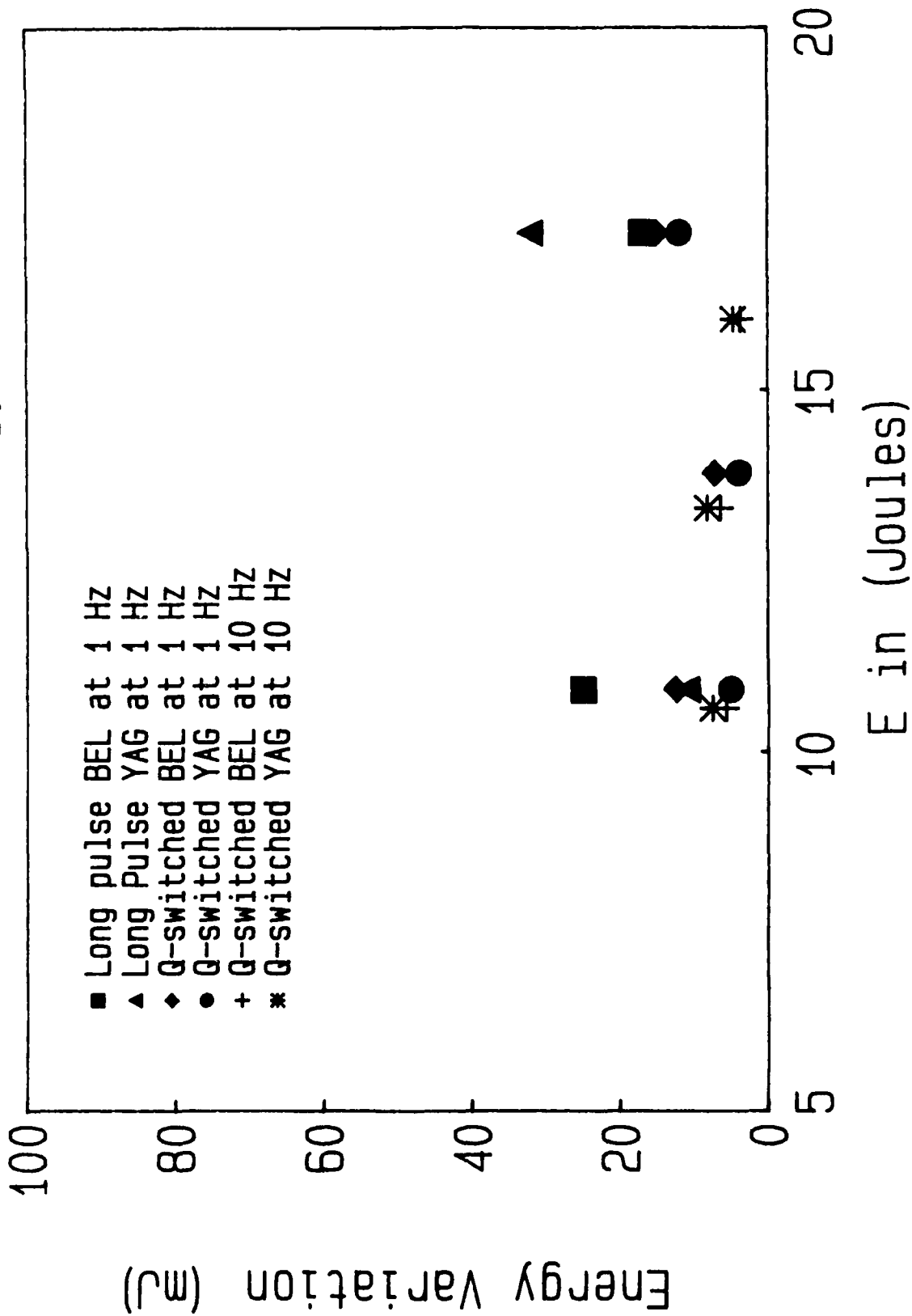
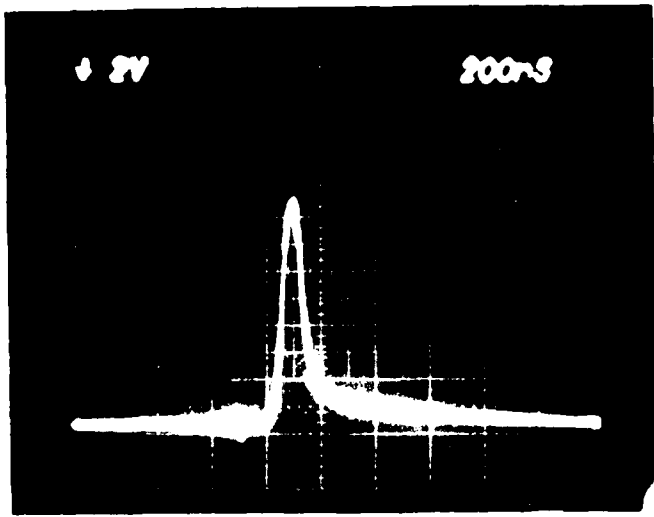
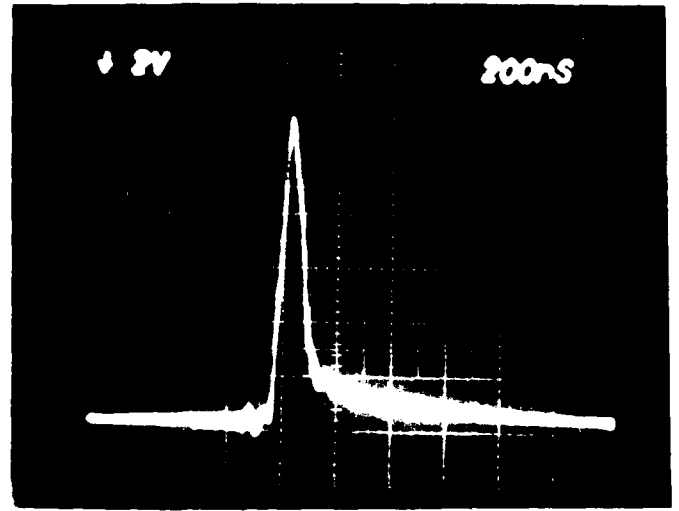


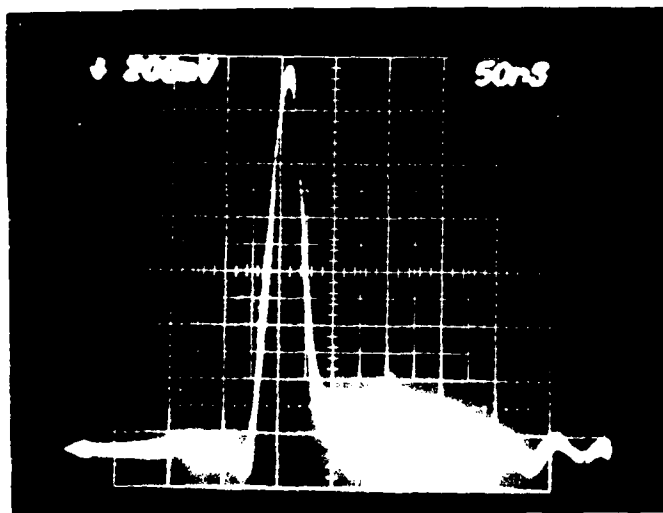
Figure 25 - Maximum to Minimum Variations



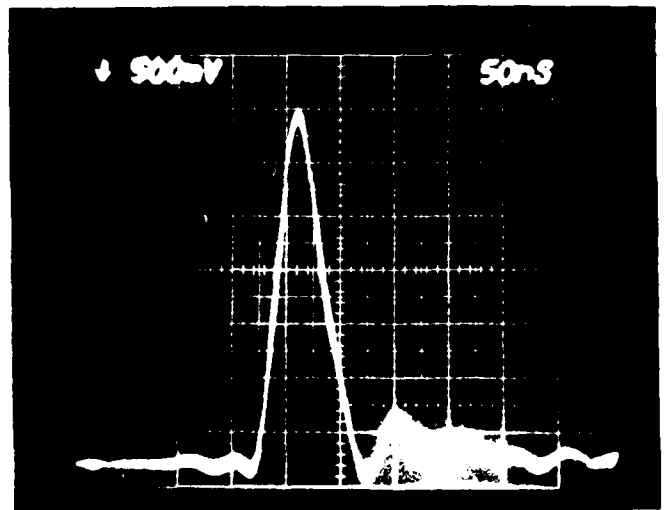
1000000 Hz, 100% amplitude



1000000 Hz, 100% amplitude



1000000 Hz, 100% amplitude



1000000 Hz, 100% amplitude

Figure 26 - 1 Hz Q-switched Pulse Widths

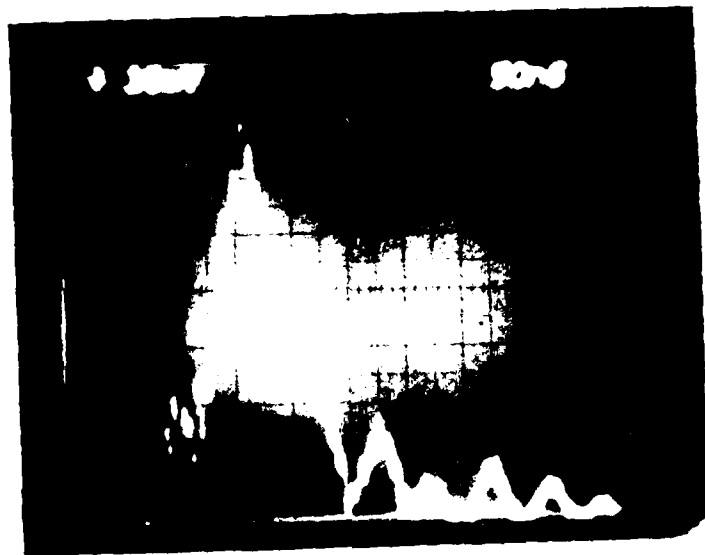


Figure 27 - Nd:BEL Q-switched Pulse Width at 10.8 J input

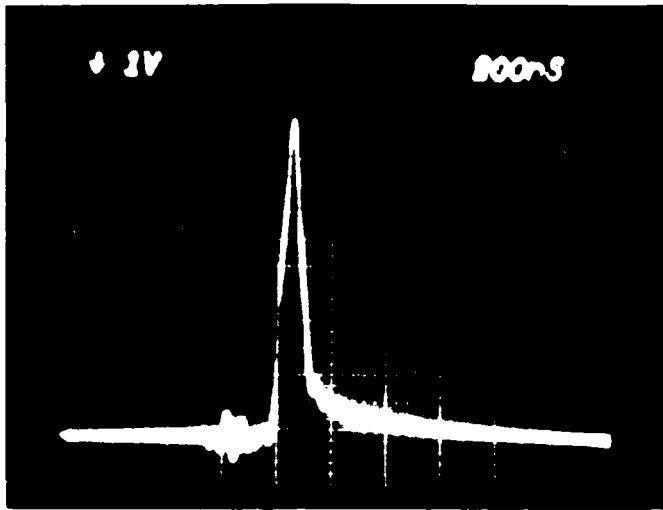


Figure 25 - 10 Hz (H-switched) Pulse Width

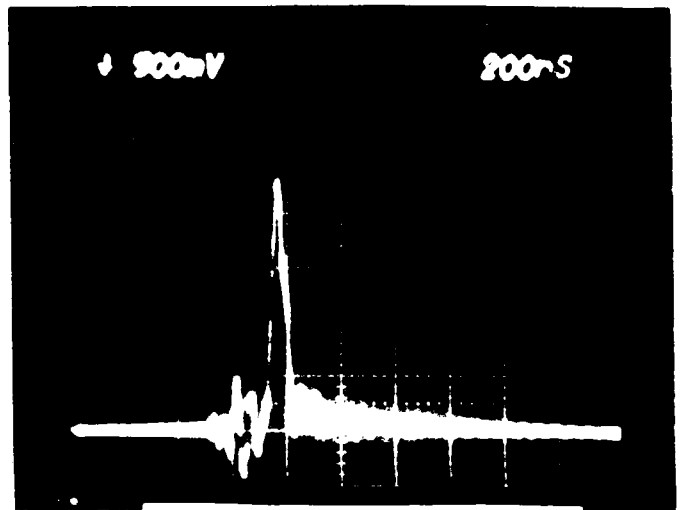


Figure 26 - 10 Hz (H-switched) Pulse Width

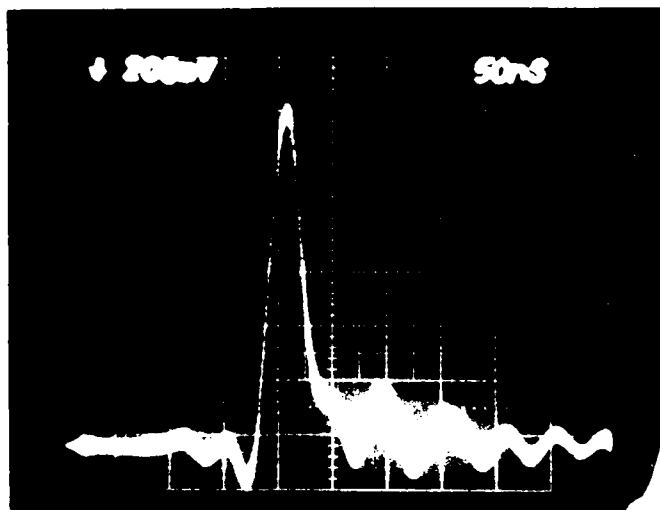


Figure 27 - 10 Hz (H-switched) Pulse Width

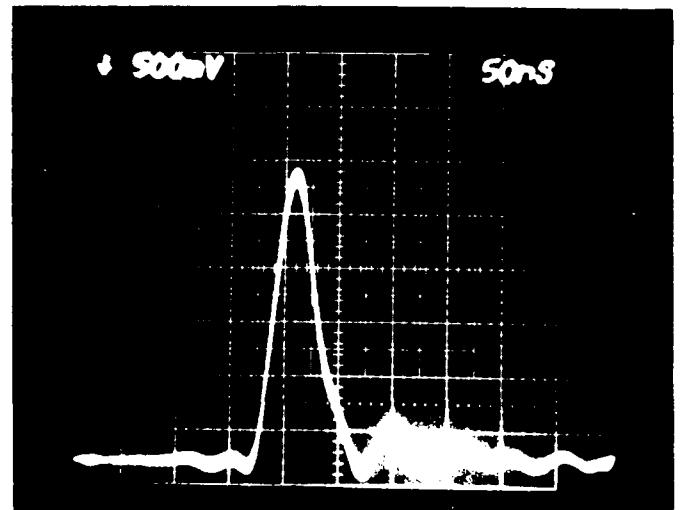


Figure 28 - 10 Hz (H-switched) Pulse Width

Figure 25 - 10 Hz (H-switched) Pulse Width

TABLE I

PHYSICAL PROPERTIES OF YAG AND BEL<sup>\*</sup>

	Lattice Constant (Angstroms)	Density (g/cm <sup>3</sup> )	Melting Point (°C)	Thermal Conductivity (W/cm-°C)	Refractive Index
BEL	a = 7.536 b = 7.347 c = 7.439	6.061	1361	0.047	1.9641 (n <sub>x</sub> ) 1.997 (n <sub>y</sub> <sup>a</sup> ) 2.0348 (n <sub>z</sub> <sup>b</sup> ) c
YAG	12.01	4.55	1970	0.13	1.823

\* Values obtained from Handbook of Laser Science and Technology, Vol. I, M. Weber, editor, CRC Press, Boca Raton, Fla., 1982.

TABLE II  
Laboratory Equipment

<u>Description</u>	<u>Number</u>
ORIEL High Reflection mirror (3 m radius of curvature)	1
Inrad Model 202-092 Q-switch	2
Inrad Model 2-016 Q-switch driver	3
PAL Kit Co. Model BP2 Pulse Generator	4
Candela FD 100 Flashlamp Driver and HVD-250A Power Supply	5
FC-20K Kigre cavity specially modified for 1/4" x 2 5/8" rod	6
Neslab RTE-4 refrigerated circulating bath	7
ORIEL 50% transmission mirror (flat)	8
Schott optical glass filters	9
Laser Precision RJP 735 probe	10
Laser Precision Rj 7200 energy ratiometer	11
Tektronix 7633 oscilloscope	12
- 7B53A dual time base	
- 7A16A amplifiers	
- C-53 camera	
Moseley Model 2D X-Y Recorder	13
Tektronix 468 digital storage oscilloscope	14
Lite Mike Model 560B detector	15
Si photodiode with Hewlett Packard 6217A power supply	16
Kentek Corp. Zap-it paper	17
Jarrell Ash .5m spectrometer	18

END

DATE

FILMED

5-88

DTIC